The Lattice Boltzmann Equation Method: Fundamentals, Place and Perspectives

R.R. Nourgaliev[†], T.G. Theofanous[†], T.N. Dinh[†] and D. Joseph[††]

[†] *Center for Risk Studies and Safety, University of California, Santa Barbara, USA*
[††] *Aerospace Engineering and Mechanics, University of Minnesota, USA*

E-mail: robert@crss.ucsb.edu; theo@theo.ucsb.edu; nam@crss.ucsb.edu; joseph@aem.umn.edu

The Lattice Boltzmann Equation (LBE) method is reviewed and analyzed. The focus is on the fundamental principles of the approach; its 'pros' and 'cons' in comparison to other methods of the computational fluid dynamics (CFD); and its perspectives as a competitive alternative computational approach for fluid dynamics. An excursion into the history, physical background and details of the theory and numerical implementation is made, with special attention paid to the method's advantages, limitations and perspectives to be a useful framework to incorporate molecular interactions for description of complex interfacial phenomena; efficiency and simplicity for modeling of hydrodynamics, comparing it to the methods, which directly solve for transport equations of macroscopic variables ("traditional CFD").

CONTENTS

1. INTRODUCTION

From its birth over 10 years ago [54], the lattice Boltzmann Equation (LBE) method has been aggressively pursued and at a pace that is strongly accelerating in the past few years. The method has found application in many different areas of computational fluid dynamics, including simulation of flows in porous media; non-ideal, binary and ternary complex fluids; microfluids; particulate and suspension flows; to name but a few (see for review [13]).

The purpose of the present paper is a comprehensive review of the LBE method. In difference to other review papers on the topic (see [13]), we would not attempt to cover all CFD areas where the LBE method has found application, but rather

focus ourselves on few fundamental principles of the method and analysis of the model's capabilities and limitations, 'pros' and 'cons' in comparison to the methods of the "traditional" CFD.

The paper is organized as a comprehensive tutorial. It starts from the discussion of the fundamental principles and origin of the approach, section 2, which includes short introduction of the kinetic theory of gases and its connection to the LBE theory; Chapman-Enskog analysis of the discrete Boltzmann equation; and derivation and discussion of the hydrodynamic equations for three most commonly used LBE models. Next, the capability and limitations of the LBE approach to model fluid-fluid multiphase flows and fluid-fluid interfaces are discussed in section 3. Finally, in section 4, we discuss the details of practical implementation of the LBE algorithms, which include introduction of the 'basic' numerical schemes utilized to solve the discrete Boltzmann equation, and comparative analysis of the method in terms of simplicity and efficiency of algorithms, and potentials for effective parallelization.

2. FUNDAMENTALS OF THE LATTICE BOLTZMANN EQUATION METHOD

To better elucidate the significance of the LBE theory, we first outline the basic pieces of the 'ground' for the LBE method, the Boltzmann equation theory, without going into details, emphasizing the major assumptions made and the domain of the theory applicability, section 2.1. Next, we describe how the 'jump' from the 'continuous' to the 'discrete' (LBE) case is made, section 2.2. The hydrodynamics of the LBE method is discussed in section 2.3, in which we outline the basic steps of the Chapman-Enskog expansion procedure and derive the 'macroscopic-level' equations for three most commonly used LBE models.

2.1. Origin of the LBE method: kinetic theory, Boltzmann equation and Enskog' extension to dense gases

Kinetic theory. The Lattice Boltzmann Equation method originates from the kinetic theory of gases. The primary variable of interest is a one-particle probability distribution function (PPDF), $f(\mathbf{r}, \mathbf{e}, t)$, so defined that $\left[f(\mathbf{r}, \mathbf{e}, t) \cdot d^3r \cdot d^3e\right]$ is the number of particles which, at time t, are located within a phase-space control element $\left[d^3r \cdot d^3e\right]$ about $\mathbf{r}$ and $\mathbf{e}$ ($\mathbf{r}$ is a particle's coordinate in physical space and $\mathbf{e}$ is a particle's velocity). Transport equation for PPDF can be expressed as [40]:

$$\left(\partial_t + \mathbf{e} \cdot \nabla_{\mathbf{r}} + \mathbf{a} \cdot \nabla_{\mathbf{e}}\right) f(\mathbf{r}, \mathbf{e}, t) = \left(\partial_t f\right)_{\text{coll}} \tag{1}$$

where $\mathbf{a}$ is the external force acting on the particle.

Boltzmann equation. To derive the Boltzmann equation from equation (1), the collision term $\left(\partial_t f\right)_{\text{coll}}$ has to be explicitly specified. Two major assumptions are made [40]: (a) only binary collisions are taken into account. This is valid if the gas is sufficiently dilute (ideal gas). (b) The velocity of a molecule is uncorrelated with its position[1] . The last assumption is known as the *assumption of molecular chaos*. Importantly, without this assumption, the collision operator $\left(\partial_t f\right)_{\text{coll}}$ would not be

[1] To be precise, there are two more assumptions made: (c) wall effects are ignored and (d) the effect of the external force on the collision cross section is neglected.

expressible in terms of f itself. Instead, it would involve a two-particle probability distribution function, which is independent of f. In general case, equation (1) is replaced by a set of N coupled equations (BBKGY equations).

Under the assumptions made, Boltzmann [8] expressed the collision term of equation (1) as[2] [11] [40] [44]:

$$(\partial_t f)_{\text{coll}} = \int d\Omega \int d^3 e^{(0)} \sigma(\Omega) \left| \mathbf{e} - \mathbf{e}^{(0)} \right| \left(f' f'^{(0)} - f f^{(0)} \right) \tag{2}$$

where Ω is the scattering angle of the binary collision $\left\{ \mathbf{e}', \mathbf{e}'^{(0)} \right\} \rightarrow \left\{ \mathbf{e}, \mathbf{e}^{(0)} \right\}$ with fixed $\mathbf{e}$; and $\sigma(\Omega)$ is the differential cross section of this collision, [40].

Boltzmann's 'H theorem'. Introducing the functional $\mathcal{H}$ as the complete integral defined by the equation

$$\mathcal{H} = \int f \ \ln f \ d\mathbf{e} \tag{3}$$

the Boltzmann 'H theorem' states that if PPDF f satisfies Boltzmann transport equation (1) and (2), then $\mathcal{H}$ is a non-increasing in time function, $\frac{d\mathcal{H}(t)}{dt} \leq 0$. This is the analog of the second law of thermodynamics, if we identify $\mathcal{H}$ with the negative of the entropy per unit volume divided by Boltzmann's constant, $\mathcal{H} = -\frac{\mathcal{S}}{V k_B}$. Thus, the 'H theorem' states that, for a fixed volume V, the entropy never decreases, [40].

Collision interval theory. Significant simplification of the collision integral eq.(2) can be made assuming that during time interval δ_t a fraction $\delta_t/\tau = \frac{1}{\tau^\star}$ of the particles in a given small volume undergo collisions, which alter the PPDF from f to the equilibrium value given by the Maxwellian:

$$f^{\text{eq}} = \frac{\rho}{(2\pi\theta)^{\mathcal{D}/2}} \exp\left[-\frac{(\mathbf{e}-\mathbf{u})^2}{2\theta} \right], \quad \theta = RT = c_s^2 \tag{4}$$

where $\mathcal{D}$, R, T, c_s, ρ and $\mathbf{u}$ are the dimension of space, gas constant, temperature, ideal gas's sound speed, macroscopic density and velocity, respectively. Thus, the collision term can be expressed in the form known as the *'BGK collision operator'* [11]:

$$(\partial_t f)_{\text{coll}} = -\frac{f - f^{\text{eq}}}{\tau} = -\frac{f - f^{\text{eq}}}{\delta_t \tau^\star} \tag{5}$$

where τ is a relaxation time[3,4].

[2] Boltzmann's derivation of the collision integral eq.(2) was rather intuitive. There is left a wide and obscure gap between Newton's equations of motion of the molecules constituting a gas and the Boltzmann equation (2). There is no proof that the Boltzmann equation is completely correct. Nevertheless, the equation is known to be valid at least as an empirical formula, which has been successfully applied to study transport properties of dilute gases [44]. The relevant equation is derived consistently according to the more general BBGKY theory (due to Bogoliubov, 1946, Kirkwood, 1947, and Grad, 1958, [49]).

[3] It is important to notice, that the BGK equation (5) is a *phenomenological equation*, because it does not follow in a logical, self-contained manner from first principles [49]. Closely related to this inhibiting phenomenological property is the domain of applicability of the equation: dilute gases in a state close to thermal equilibrium. The inaccuracy of the BGK equation is enhanced when one treats the equation by a method similar to the Chapman-Enskog method [44].

[4] It is instructive to note that the 'H theorem' for BGK equation also holds, [44].

Dense gases. In real ('dense', 'non-ideal') gases, the mean free path is comparable with molecular dimensions. Thus, additional mechanism for momentum and energy transfer has to be considered. Beside the transfer of molecular properties *between* collisions, a transfer *during* the collision event must be accounted for [11]. This collisional transfer has been considered by Enskog (1921), who approximated the effects of the exclusion volume of the molecules under constant temperature conditions by explicitely adding the *'exclusion volume'* term to the Boltzmann's collision integral. The most commonly used (approximate) form of this term is

$$(\partial_t f)_{\text{coll, Enskog}} = (\partial_t f)_{\text{coll, Boltzmann}} - \underbrace{f^{\text{eq}} \mathsf{b}\rho\chi(\mathbf{e}-\mathbf{u})\cdot\nabla\ln(\rho^2\chi)}_{\substack{\text{Approximation}\\ \text{of the Enskog's}\\ \text{'exclusion}\\ \text{volume' term}}} \tag{6}$$

where $\mathsf{b} = \frac{2\pi \mathsf{d}}{3m}$ is the second virial coefficient in the virial equation of state; χ is the increase in collision probability due to the increase in fluid density, which has the following asymptotic form [11]:

$$\chi = 1 + \frac{5}{8}\mathsf{b}\rho + 0.2869(\mathsf{b}\rho)^2 + 0.1103(\mathsf{b}\rho)^3 + ... \tag{7}$$

d and m are the diameter and mass of the molecules, respectively. Combination of eqs.(1), (2) and (6), known as the 'Enskog equation' in the literature [29], has recently been used by Luo in his 'unified theory of lattice Boltzmann models for nonideal gases'[5], [50].

It is instructive to note that, in his derivation, Enskog employed 'hard-sphere model', which has advantage of mathematical simplicity, since many-body interactions are neglected (collisions are instantaneous). This model is, however, not appropriate for real gases under high pressure, because the molecules are in the force field of others during a large part of their motion, and multiple encounters are not rare[6], [11].

"HSD" model. Recently, He, Shan and Doolen [31] proposed the following approximate model of dense gases. The starting point is the Boltzmann equation with the BGK collision operator:

$$\partial_t f + \mathbf{e}\cdot\nabla_{\mathbf{r}} f + \mathbf{a}\cdot\nabla_{\mathbf{e}} f = -\frac{f - f^{\text{eq}}}{\tau} \tag{8}$$

In order to evaluate the forcing term, the derivative $\nabla_{\mathbf{e}} f$ has to be explicitely given. The following assumption is made:

$$\nabla_{\mathbf{e}} f \approx \nabla_{\mathbf{e}} f^{\text{eq}} \tag{9}$$

[5] In his model, Luo employed the BGK collision operator multiplied by factor χ, $(\partial_t f)_{\text{coll, Boltzmann}} = -\frac{\chi(f-f^{\text{eq}})}{\tau}$.

[6] The reason why Enskog preferred 'hard-sphere model' is that at that time it was believed that the assumption of molecular chaos for rigid spherical molecules is valid even at high densities. This assumption is appropriate only in the case of uniform steady state [11], while for non-uniform state (for example, in the regions of fluid-solid boundaries and fluid-gas interface), there may be some correlation between velocities of neighbouring molecules, because of their recent interaction with each other or with the same neighbours.

which is due to the fact that $f^{\rm eq}$ is the leading part of the distribution function f ('an assumption of small deviation from the equilibrium'). Substituting the Maxwellian eq.(4) into eq.(9), the following equation is obtained:

$$\partial_t f + \mathbf{e}\cdot\nabla_{\mathbf{r}} f = -\frac{f-f^{\rm eq}}{\tau} + \frac{(\mathbf{F}+\mathbf{g})\cdot(\mathbf{e}-\mathbf{u})}{\rho c_s^2} f^{\rm eq} \tag{10}$$

where $\mathbf{F}$ and $\mathbf{g}$ are the effective molecular interaction and gravity forces, respectively, $\mathbf{a} = \frac{\mathbf{F}+\mathbf{g}}{\rho}$. The effective molecular interaction force $\mathbf{F}$ is designed to simulate non-ideal gas effects.

$$\mathbf{F} = \underbrace{-\rho\nabla\mathcal{V}}_{\substack{\text{Intermolecular}\\ \text{attraction by}\\ \text{mean-field}\\ \text{approximation}}} - \underbrace{\mathsf{b}\rho^2 c_s^2 \chi\cdot\nabla\ln(\rho^2\chi)}_{\substack{\text{Enskog's exclusion volume effect}\\ \text{of the molecules on the}\\ \text{equilibrium properties of dense}\\ \text{gases}}} \tag{11}$$

The intermolecular attraction potential[7] $\mathcal{V}$ is expressed as

$$\mathcal{V}(\mathbf{r}_0) = \int_{r_{01}>\mathsf{d}} u_{\rm attr}(r_{01})\ \rho(\mathbf{r}_1)\ d\mathbf{r}_1 \tag{12}$$

where $u_{\rm attr}(r_{01})$ is the attractive component of the intermolecular pairwise potential of molecules '0' and '1' separated by distance $r_{01} = |\mathbf{r}_0 - \mathbf{r}_1|$. The next step is to expand density about $\mathbf{r}_0$. Assuming that the density gradients are small, the intermolecular attraction potential is expressed as

$$\mathcal{V} = -2\mathsf{a}\rho - \kappa\nabla^2\rho \tag{13}$$

where constants a and κ are given by

$$\mathsf{a} = -\frac{1}{2}\int_{r>\mathsf{d}} u_{\rm attr}(r)\ d\mathbf{r}; \quad \kappa = -\frac{1}{6}\int_{r>\mathsf{d}} r^2 u_{\rm attr}(r)\ d\mathbf{r} \tag{14}$$

with κ determining the strength of the surface tension. Elucidating the thermodynamical aspects of this model, the intermolecular force $\mathbf{F}$ can be cast into the following form [32]:

$$\mathbf{F} = -\nabla P^\star + \underbrace{\kappa\rho\nabla\nabla^2\rho}_{\substack{\text{Force associated}\\ \text{with surface}\\ \text{tension}}}$$

$$P^\star(\rho) = \mathsf{b}\rho^2 c_s^2\chi - \mathsf{a}\rho^2 = \underbrace{P - \rho c_s^2}_{\substack{\text{'Non-ideal part'}\\ \text{of the equation}\\ \text{of state}}} \quad ; \quad P = \rho c_s^2(1+\mathsf{b}\rho\chi) - \mathsf{a}\rho^2 \tag{15}$$

[7] To certain extent, implementation of the intermolecular attraction potential $\mathcal{V}$ allows to effectively compensate for some limitations of the Enskog' 'hard-sphere' model.

Setting $\mathsf{b} = \frac{\chi-1}{\rho\chi}$, the van der Waals equation of state is obtained:

$$P = \frac{\rho c_s^2}{1-\mathsf{b}\rho} - \mathsf{a}\rho^2 \tag{16}$$

2.2. From Boltzmann equation to Lattice Boltzmann Equation

2.2.1. Heuristic approach

Historically, the 'classical' LB equation has been developed empirically, with basic idea borrowed from the cellular automata fluids [28] and [85]. The physical space of interest is filled with regular lattice populated by discrete particles. Particles 'jump' from one site of the lattice to another with discrete particle velocities $\mathbf{e}_a$, $(a = 0, ..., b$, where b is the total number of possible molecule's directions), and colliding with each other at the lattice nodes, Figs.1a,1b. The lattice geometry (a set of possible particle velocities) should obey certain symmetry requirements (see Appendix A), which are compelling in order to recover rotational invariance of the momentum flux tensor at a macroscopic level [85].

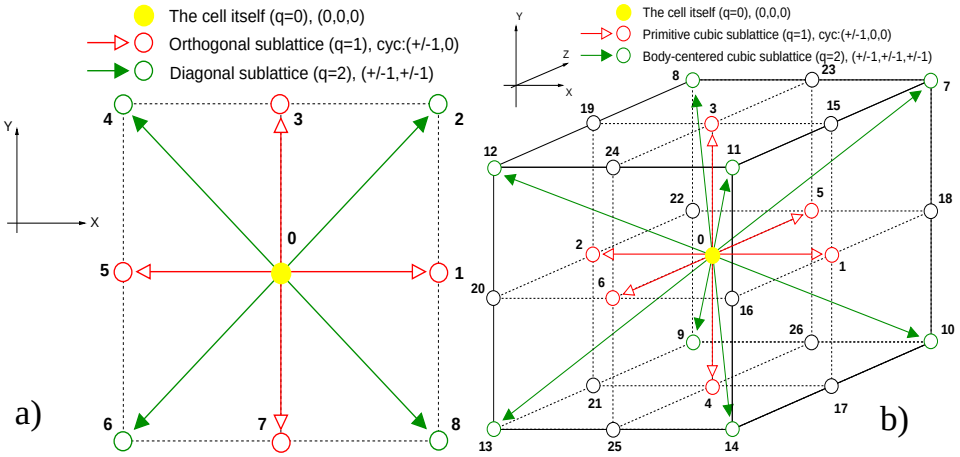

FIG. 1a. Lattice geometry and velocity vectors of the two-dimensional nine-speed D_2Q_9 model.

FIG. 1b. Lattice geometry and velocity vectors of the three-dimensional fifteen-speed D_3Q_{15} model.

In effect, for the LBE method, this corresponds to the following formal discretization of the phase space and Boltzmann equation:

$$\begin{aligned} &\text{a)}\ f \rightarrow f_a \\ &\text{b)}\ \mathbf{e} \rightarrow \mathbf{e}_a \\ &\text{c)}\ f^{\mathrm{eq}} \rightarrow f_a^{\mathrm{eq}} = A_a + B_a e_{a_i} u_i + C_a u^2 + D_a e_{a_i} e_{a_j} u_i u_j \end{aligned} \tag{17}$$

where the form of the discrete equilibrium distribution function is inspired by the following constant-temperature and small velocity (low-Mach-number) approxima-

tion of the Maxwellian eq.(4)

$$f^{eq} \approx \frac{\rho \cdot \exp\left[-\frac{\mathbf{e}^2}{2c_s^2}\right]}{\left(2\pi c_s^2\right)^{\mathcal{D}/2}} \times \left\{1 + \frac{(\mathbf{e}\cdot\mathbf{u})}{c_s^2} + \frac{(\mathbf{e}\cdot\mathbf{u})^2}{2(c_s^2)^2} - \frac{\mathbf{u}^2}{2c_s^2}\right\} + \mathcal{O}(\mathbf{u}^3) \tag{18}$$

Thus, the lattice Boltzmann BGK equation is heuristically postulated as[8]

$$\underbrace{\partial_t f_a + e_{a_j}\partial_j f_a}_{\text{Advection operator, } \mathcal{A}(f_a)} = \underbrace{-\frac{f_a - f_a^{\text{eq}}}{\tau} + \frac{a_j \cdot (e_{a_j} - u_j)}{c_s^2} f_a^{\text{eq}}}_{\text{Collision operator, } \Omega(f_a)} \tag{19}$$

At this point, a principal departure from the actual kinetic theory must be highlighted. As we show further below, if the fluid being modeled is to retain its speed of sound, the solution of eq.(19) is impossible for all practical purposes. As a consequence, compressibility effects are outside the realm of the LBE method; c_s is retained, however, with a totally different meaning and role - that of a pseudo compressibility parameter that allows the solution to relax to the appropriate incompressible viscous solution. Rather than sound speed, let us call, therefore, c_s by the name *"Lattice-Internal Speed"* (*"LIS"*). While this departs from normal usage, its adoption, we believe, will clear up an enormous conceptual barrier for the newcomers and uninitiated.

The coefficients A_a, B_a, C_a and D_a of the 'Chapman-Enskog' expansion for f_a^{eq}, eq.(17), are 'tuned' to recover mass, momentum conservation and viscous stress tensor during the multiscale Chapman-Enskog perturbative expansion procedure[9] (see section 2.3 and Appendix B).

Eqs.(19) are the coupled system of Hamilton-Jacobi equations, with Hamiltonian $e_{a_j}\partial_j f_a$, and the 'coupling' source term given by the collision operator. This system can be solved by any appropriate numerical scheme (see section 4).

Non-dimensional form. To cast the discrete Boltzmann equation (19) into the non-dimensional form, one must introduce the following characteristic scales:

Characteristic length scale:	L
Characteristic velocity:	U_0
Reference density:	ρ_{r}
Molecular mean free path:	λ

(20)

[8] For approximation of the external forcing term, we use the 'HSD' assumption eq.(9).

[9] In the case of the 'thermal' LBE, it is also required to conserve energy, which would entail addition of the expansion terms in the Taylor series eqs.(17) and (18).

Using these scales, the variables utilized in the LBE theory are non-dimensionalized as

$$
\begin{array}{lll}
\multicolumn{3}{c}{\textit{Non-dimensional variables:}} \\
\textit{PDF:} & \hat{f}_a & = \frac{f_a}{\rho_r} \\
\textit{Molecular velocity:} & \hat{e}_{a_i} & = \frac{e_{a_i}}{\mathsf{U}_0} \\
\textit{Time:} & \hat{t} & = \frac{t\mathsf{U}_0}{\mathsf{L}} \\
\textit{Length:} & \hat{\mathbf{r}} & = \frac{\mathbf{r}}{\mathsf{L}} \\
\textit{Density:} & \hat{\rho} & = \frac{\rho}{\rho_r} \\
\textit{Macroscopic velocity:} & \hat{u}_i & = \frac{u_i}{\mathsf{U}_0} \\
\textit{Lattice internal speed:} & \hat{c}_s & = \frac{c_s}{\mathsf{U}_0} \\
\textit{Body force:} & \hat{a}_j & = \frac{a_j \mathsf{L}}{\mathsf{U}_0^2} = \frac{1}{\mathsf{Fr}} \\
\textit{Kinematic viscosity:} & \hat{\nu} & = \frac{\nu}{\mathsf{U}_0 \mathsf{L}} = \frac{1}{\mathsf{Re}}
\end{array}
\tag{21}
$$

To make a non-dimensional relaxation time, we will use the Knudsen number defined as a ratio of the molecular mean free path λ to the flow characteristic length scale L:

$$\varepsilon = \frac{\lambda}{\mathsf{L}} \tag{22}$$

Defining the collision time as $\mathsf{t_c} \equiv \frac{\lambda}{\mathsf{U}_0}$, the dimensionless relaxation time is

$$\hat{\tau} = \frac{\tau}{\mathsf{t_c}} = \frac{\tau \mathsf{U}_0}{\lambda} \tag{23}$$

With this dimensionalization introduced, the discrete Boltzmann equation (19) is transformed into the following non-dimensional equation:

$$\partial_{\hat{t}} \hat{f}_a + \hat{e}_{a_j} \partial_{\hat{j}} \hat{f}_a = -\frac{\hat{f}_a - \hat{f}_a^{\mathrm{eq}}}{\varepsilon \hat{\tau}} + \frac{\hat{a}_j \cdot (\hat{e}_{a_j} - \hat{u}_j)}{\hat{c}_s^2} \hat{f}_a^{\mathrm{eq}} \tag{24}$$

For the most of the paper, for compactness, the hat $\hat{(\cdot)}$ is omitted; and, unless explicitely specified, all variables are assumed to be non-dimensional.

2.2.2. 'Consistent discretization'

Recent studies by He and Luo [33] [34] pioneer another way to establish the LBE theory. In particular, He and Luo [34] demonstrated that the lattice Boltzmann equation can be viewed as a *special finite-difference approximation* of the Boltzmann equation. The chief idea and motivation are to provide a sound theoretical foundation for a transition from the 'continuous' Boltzmann equation to the LBE, which involves the choice of the discrete particle velocities (structure of the lattice) and the choice of the coefficients of expansion for equilibrium distribution function, eq.(17). There are two major ingredients in the procedure by He and Luo, discussed below.

Time discretization. Eq.(8) is integrated over a time step δ_t:

$$
\begin{aligned}
f\left(\mathbf{r} + \mathbf{e}\cdot\delta_t, \mathbf{e}, t+\delta_t\right) - f\left(\mathbf{r}, \mathbf{e}, t\right) = &- \int_t^{t+\delta_t} \frac{f - f^{\mathrm{eq}}}{\tau} dt + \\
&+ \int_t^{t+\delta_t} \frac{\mathbf{a}\cdot(\mathbf{e}-\mathbf{u})}{c_s^2} f^{\mathrm{eq}}
\end{aligned}
\tag{25}
$$

The first integral in the collision operator is treated explicitely, using the first-order approximation, while the second one can be treated using the trapezoidal implicit scheme [31], which, in order to regain the expliciteness of the method, entails the following variable transformation:

$$h = f - \frac{\mathbf{a}\cdot(\mathbf{e}-\mathbf{u})}{2c_s^2} f^{\mathrm{eq}}\delta_t \tag{26}$$

Thus, the first-order time discretization yields the following Boltzmann equation:

$$\begin{array}{c} h\left(\mathbf{r}+\mathbf{e}\cdot\delta_t,\mathbf{e},t+\delta_t\right)-h\left(\mathbf{r},\mathbf{e},t\right)=-\frac{h\left(\mathbf{r},\mathbf{e},t\right)-h^{\mathrm{eq}}\left(\mathbf{r},\mathbf{e},t\right)}{\tau} \\ \text{where} \quad h^{\mathrm{eq}}=\left[1-\frac{\mathbf{a}\cdot(\mathbf{e}-\mathbf{u})}{2c_s^2}\delta_t\right] f^{\mathrm{eq}} \end{array} \tag{27}$$

Phase space discretization. This step establishes the structure of the lattice and the form of the equilibrium distribution function.

Connection of the Boltzmann equation to the hydrodynamics is realized through the integration in the particle momentum space[10]:

$$\begin{array}{lll} \rho=\int[f]\,d\mathbf{e}; & \rho\mathbf{u}=\int[f\cdot\mathbf{e}]\,d\mathbf{e}; & \rho\mathcal{E}=\frac{1}{2}\int\left[f\cdot(\mathbf{e}-\mathbf{u})^2\right]d\mathbf{e} \\ \rho=\int[f^{\mathrm{eq}}]\,d\mathbf{e}; & \rho\mathbf{u}=\int[f^{\mathrm{eq}}\cdot\mathbf{e}]\,d\mathbf{e}; & \rho\mathcal{E}=\frac{1}{2}\int\left[f^{\mathrm{eq}}\cdot(\mathbf{e}-\mathbf{u})^2\right]d\mathbf{e} \end{array} \tag{29}$$

with the kinetic energy $\mathcal{E}$ given by

$$\mathcal{E}=\frac{\mathcal{D}_0}{2}RT=\frac{\mathcal{D}_0}{2}c_s^2=\frac{\mathcal{D}_0}{2}N_A k_B T \tag{30}$$

where N_A and k_B are the Avogadro's number and the Boltzmann constant, respectively. $\mathcal{D}_0$ is the number of degrees of freedom of a particle ($\mathcal{D}_0 = 3$ for monoatomic gas).

To derive a consistent LBE scheme, the integration in momentum space eq.(29) has to be approximated by the following quadrature [34]:

$$\int\psi(\mathbf{e})f^{\mathrm{eq}}(\mathbf{r},\mathbf{e},t)d\mathbf{e}\approx\sum_a\mathcal{W}_a\,\psi(\mathbf{e}_a)f_a^{\mathrm{eq}}(\mathbf{r},\mathbf{e}_a,t) \tag{31}$$

where $\psi(\mathbf{e}) = [1; e_i; (e_ie_j); (e_ie_je_k); ...]$ and $\mathcal{W}_a$ are the polynomials of $\mathbf{e}$ and the 'weight' coefficient of the quadrature, respectively. Eq.(31) corresponds to the following 'link' of the LBE to hydrodynamics:

$$\begin{array}{lll} \rho=\sum_a f_a; & \rho\mathbf{u}=\sum_a f_a\cdot\mathbf{e}_a; & \rho\mathcal{E}=\frac{1}{2}\sum_a f_a\cdot(\mathbf{e}_a-\mathbf{u})^2 \\ \rho=\sum_a f_a^{\mathrm{eq}}; & \rho\mathbf{u}=\sum_a f_a^{\mathrm{eq}}\cdot\mathbf{e}_a; & \rho\mathcal{E}=\frac{1}{2}\sum_a f_a^{\mathrm{eq}}\cdot(\mathbf{e}_a-\mathbf{u})^2 \end{array} \tag{32}$$

where

$$f_a(\mathbf{r},t)\equiv\mathcal{W}_a\ f(\mathbf{r},\mathbf{e}_a,t); \qquad f_a^{\mathrm{eq}}(\mathbf{r},t)\equiv\mathcal{W}_a\ f^{\mathrm{eq}}(\mathbf{r},\mathbf{e}_a,t) \tag{33}$$

[10] In the case of the transformation eq.(26), f is substituted by h, and the first momentum is modified as

$$\rho\mathbf{u}-\tfrac{1}{2}\rho\mathbf{a}\delta_t=\int[h\cdot\mathbf{e}]\,d\mathbf{e}; \qquad \rho\mathbf{u}-\tfrac{1}{2}\rho\mathbf{a}\delta_t=\int[h^{\mathrm{eq}}\cdot\mathbf{e}]\,d\mathbf{e} \tag{28}$$

Now, a task is to properly specify the abscissas of the quadrature eq.(31), or, in other words, the 'structure' ('symmetry') of the lattice. To do that, one must impose a set of constraints for this 'structure'. These constraints are formulated based on the Chapman-Enskog procedure to 'link' the Boltzmann equation to the Navier-Stokes equations, see section 2.3.1, which involves the following moments of the equilibrium distribution function:

$$\begin{array}{ll} \textit{Mass conservation:} & \psi(\mathbf{e}) = 1;\ e_i;\ \text{and } e_i e_j \\ \textit{Momentum conservation:} & \psi(\mathbf{e}) = 1;\ e_i;\ e_i e_j;\ \text{and } e_i e_j e_k \\ \textit{Energy conservation:} & \psi(\mathbf{e}) = 1;\ e_i;\ e_i e_j;\ e_i e_j e_k;\ \text{and } e_i e_j e_k e_l \end{array} \tag{34}$$

Thus, the basic idea is that with the chosen abscissas of the quadrature eq.(31), the moments of f_a^{eq}, eq.(34), should be calculated exactly. With this, the Chapman-Enskog procedure is intact, and it is argued that the framework of the lattice Boltzmann equation can rest on that of the Boltzmann equation, and the rigorous results of the Boltzmann equation can be extended to the LBE via this explicit connection [33]. It is important to note that the Maxwell-Boltzmann equilibrium distribution function f^{eq} is an exact solution of the Chapman-Enskog's zero-order approximation of the Boltzmann equation [40]. In finding the abscissas of the quadrature eq.(31), however, instead of the exact Maxwellian, its constant-temperature and low-Mach-number approximation eq.(18) is utilized, [34], with which no rigorous link to the Navier-Stokes equations is available. Moreover, this is exactly the reason why the Boltzmann's "H theorem" does not hold for the LBE. Therefore, this procedure does not provide substitute for the Chapman-Enskog multiscale perturbative expansion procedure, section 2.3.1.

The details of the procedure to find the required abscissas of the quadrature and corresponding approximations of the Maxwellian are given in [34] for two-dimensional 6-, 7- and 9-bit and three-dimensional 27-bit lattice models. It is important to note that with this procedure, the 'weighting' coefficients for the 'composing' sublattices and the coefficients of the equilibrium distribution function are exactly the same as those of the 'heuristic' LBE, summarized in Appendices A and B, providing that[11] $c_s^2 = \frac{\Upsilon^{(4)}}{\Upsilon^{(2)}}$, [35].

2.3. Derivation of the hydrodynamic equations from the Lattice Boltzmann Equation

2.3.1. Chapman-Enskog expansion method

The purpose of the Chapman-Enskog method is to solve Boltzmann equation by successive approximations. This yields only a particular type of solutions, namely, those that depend on the time implicitely through the local density, velocity and temperature, $f(t) = f\ (\ \rho(t), \mathbf{u}(t), T(t)\ )$ - the 'Chapman-Enskog *ansatz*', [40]. In

[11] Note, that, in general, in the 'heuristic' LBEs, the lattice symmetry parameters $\Upsilon^{(4)}$ and $\Upsilon^{(2)}$ are adjustable, with free parameter w_0, allowing to vary lattice sound speed. For D_2Q_9, the requirement $c_s^2 = \frac{\Upsilon^{(4)}}{\Upsilon^{(2)}}$ is satisfied with $w_0 = \frac{4}{9}$.

the present section, we outline the basic steps of the procedure, applied to the isothermal discrete Boltzmann equation (24)[12].

First, introduce the following formal expansion of the discrete probability distribution function:

$$f_a = f_a^{(0)} + \varepsilon f_a^{(1)} + \varepsilon^2 f_a^{(2)} + ... = \sum_{k=0}^{\infty} \varepsilon^k f_a^{(\mathrm{k})} \tag{36}$$

where ε is a Knudsen number, eq.(22). In the Chapman-Enskog theory, this parameter is introduced to keep track of the order of the terms in the series. The functions $f_a^{(\mathrm{k})}$ are defined in such a way that $f_a^{(\mathrm{k})}$ gets smaller and smaller as k increases. The main achievement of the Chapman-Enskog expansion is to provide a way of defining $f_a^{(\mathrm{k})}$ that is both consistent and practicable [40]. It is required that the first three moments of the zeroth approximation reproduce macroscopic density, velocity and kinetic energy, while corresponding moments of the higher-order terms are zero:

$$\begin{array}{lll} \sum_a f_a^{(0)} = \rho; & \sum_a f_a^{(0)} e_{a_i} = \rho u_i & \frac{1}{2}\sum_a f_a^{(0)} \cdot (e_{a_i} - u_i)^2 = \rho\mathcal{E}; \\ \sum_a f_a^{(\mathrm{n})} = 0; & \sum_a f_a^{(\mathrm{n})} e_{a_i} = 0; & \sum_a f_a^{(\mathrm{n})} e_a^2 = 0; \quad n > 0 \end{array} \tag{37}$$

Thus, eqs.(32) are satisfied[13].

LBE conservation laws. Substituting expansion eq.(36) into eq.(24) and taking the first 'discrete moment' ($\sum_a$ eq.(24)) result in the mass conservation equation

$$\underline{\textit{Mass conservation law:}} \qquad \partial_t \rho + \partial_j \rho u_j = 0 \tag{38}$$

Taking the second 'discrete moment' ($\sum_a$ eq.(24) $\times\, e_{a_i}$) yields the momentum conservation law:

$$\partial_t \rho u_i = -\partial_j \sum_{n=0}^{\infty} \varepsilon^n \sum_a e_{a_i} e_{a_j} f_a^{(\mathrm{n})} + \frac{a_j}{c_s^2} \left(\sum_a f_a^{\mathrm{eq}} e_{a_i} e_{a_j} - \rho u_i u_j \right) \tag{39}$$

Introducing the n^{th} approximation of the pressure tensor as

$$\mathcal{P}_{i,j}^{(\mathrm{n})} \equiv \sum_a (e_{a_i} - u_i)(e_{a_j} - u_j) f_a^{(\mathrm{n})} \tag{40}$$

[12] To avoid using expansions:

$$f_a(\mathbf{r} + \mathbf{e}_a \delta_t, t + \delta_t) = \sum_{k=0}^{\infty} \frac{\varepsilon^n}{n!} \mathsf{D}_t^n f_a(\mathbf{r}, t); \quad \mathsf{D}_t \equiv (\partial_t + \mathbf{e}_a \cdot \nabla) \tag{35}$$

traditionally employed to evaluate 'stream-and-collide' advection operator, $\mathcal{A}(f_a) = f_a(\mathbf{r} + \mathbf{e}_a\delta_t, t + \delta_t) - f_a(\mathbf{r}, t)$, [30] [77], we assume that high-order finite-difference scheme is applied to the $\mathcal{A}(f_a) = \partial_t f_a + e_{a_j}\partial_j f_a$ (see section 4).

[13] Importantly, this is not the only way to satisfy these equations, but it is definitely a possible one.

the momentum conservation equation (39) is re-arranged into the following form[14]:

$$\underline{\textit{Momentum conservation law:}}$$
$$\partial_t \rho u_i + \partial_j \rho u_i u_j = -\partial_j \sum_{n=0}^{\infty} \varepsilon^n \mathcal{P}_{i,j}^{(\mathrm{n})} + \underbrace{\frac{a_j}{c_s^2}\left(\Pi_{i,j}^{\mathrm{eq}} - \rho u_i u_j\right)}_{F_{i,j}} \tag{41}$$

To derive the kinetic energy conservation equation, substitute expansion eq.(36) into eq.(24), then multiply it by $\frac{e_a^2}{2}$, and sum over all molecule directions. In addition, make use of the following equation:

$$\partial_t \sum_a f_a^{(0)} \frac{e_a^2}{2} = \partial_t \rho \mathcal{E} + u_i \partial_t \rho u_i - \frac{u^2}{2} \partial_t \rho \tag{42}$$

coming from the definition of the kinetic energy eq.(32) and constraints eq.(37). Also, introduce the n^{th} approximation of the heat flux as

$$\mathcal{Q}_i^{(\mathrm{n})} \equiv \frac{1}{2} \sum_a (e_{a\,i} - u_i)(e_{a_j} - u_j)^2 f_a^{(\mathrm{n})} \tag{43}$$

which allows to write the energy conservation equation as

$$\underline{\textit{Kinetic energy conservation law:}}$$
$$\partial_t \rho \mathcal{E} + \partial_j \rho \mathcal{E} u_j = -\partial_j \sum_{n=0}^{\infty} \varepsilon^n \mathcal{Q}_j^{(\mathrm{n})} - \partial_j u_i \cdot \sum_{n=0}^{\infty} \varepsilon^n \mathcal{P}_{i,j}^{(\mathrm{n})}$$
$$+ \underbrace{\frac{a_j}{c_s^2}\left[\sum_a f_a^{(\mathrm{eq})} \left(\frac{(e_{a_j} - u_j)e_a^2}{2} - e_{a\,i} e_{a_j} u_i\right) + \rho u_j u^2\right]}_{Q_j} \tag{44}$$

LBE successive approximation. To obtain a consistent scheme of successive approximation, $f_a^{(\mathrm{n})}$ is defined in such a way that if all $f_a^{(\mathrm{k})}$, $\mathcal{P}_{i,j}^{(\mathrm{k})}$ and $\mathcal{Q}_j^{(\mathrm{k})}$ are neglected for $k > n$, than we have the n^{th} approximation to the distribution function and to the hydrodynamic equations. To find such a definition, we decompose eq.(24) into successive equations for $f_a^{(\mathrm{n})}$ in the following manner.

1. Introduce expansion:

$$\mathsf{D} f_a = \mathsf{D} f_a^{(0)} + \varepsilon \mathsf{D} f_a^{(1)} + \varepsilon^2 \mathsf{D} f_a^{(2)} + \ldots \tag{45}$$

Consistency of this expansion with eq.(36) follows from the linearity of the operator $\mathsf{D} \equiv e_{a_j} \partial_j$.

2. Consider $\partial_t f_a$. Due to the 'Chapman-Enskog *ansatz*', f_a depends on time implicitly, only through the ρ, ρu_i and $\rho\mathcal{E}$. Thus,

$$\frac{\partial f_a}{\partial t} = \frac{\partial f_a}{\partial \rho}\frac{\partial \rho}{\partial t} + \frac{\partial f_a}{\partial \rho u_i}\frac{\partial \rho u_i}{\partial t} + \frac{\partial f_a}{\partial \rho \mathcal{E}}\frac{\partial \rho \mathcal{E}}{\partial t} \tag{46}$$

[14] Note, the following notation is in use: $\Pi_{i,j}^{\mathrm{eq}} \equiv \sum_a f_a^{(\mathrm{eq})} e_{a\,i} e_{a_j}$.

To expand eq.(46) into infinite series in powers of ε, expand $\frac{\partial f_a}{\partial \rho}$, $\frac{\partial f_a}{\partial \rho u_i}$ and $\frac{\partial f_a}{\partial \rho \mathcal{E}}$ as

$$\begin{array}{lll} \frac{\partial f_a}{\partial \rho} & = \frac{\partial f_a^{(0)}}{\partial \rho} & +\varepsilon \frac{\partial f_a^{(1)}}{\partial \rho} \quad +\varepsilon^2 \frac{\partial f_a^{(2)}}{\partial \rho} + ... \\ \frac{\partial f_a}{\partial \rho u_i} & = \frac{\partial f_a^{(0)}}{\partial \rho u_i} & +\varepsilon \frac{\partial f_a^{(1)}}{\partial \rho u_i} \quad +\varepsilon^2 \frac{\partial f_a^{(2)}}{\partial \rho u_i} + ... \\ \frac{\partial f_a}{\partial \rho \mathcal{E}} & = \frac{\partial f_a^{(0)}}{\partial \rho \mathcal{E}} & +\varepsilon \frac{\partial f_a^{(1)}}{\partial \rho \mathcal{E}} \quad +\varepsilon^2 \frac{\partial f_a^{(2)}}{\partial \rho \mathcal{E}} + ... \end{array} \tag{47}$$

The expansions for time derivatives $\partial_t \rho$, $\partial_t \rho u_i$ and $\partial_t \rho \mathcal{E}$ must be defined to be consistent with the conservation laws eqs.(38), (41) and (44). Thus, the definition of $\frac{\partial_n}{\partial t}$ is taken from the n^{th} approximation to the conservation laws:

Mass conservation:

$$\begin{array}{ll} \partial_{t_0} \rho & \equiv -\partial_j \rho u_j \\ \partial_{t_n} \rho & \equiv 0; \qquad (n > 0) \end{array} \tag{48}$$

Momentum conservation:

$$\begin{array}{ll} \partial_{t_0} \rho u_i & \equiv -\partial_j \rho u_i u_j - \partial_j \mathcal{P}_{i,j}^{(0)} + F_{i,j} \\ \partial_{t_n} \rho u_i & \equiv -\partial_j \mathcal{P}_{i,j}^{(\mathrm{n})}; \qquad (n > 0) \end{array} \tag{49}$$

Energy conservation:

$$\begin{array}{ll} \partial_{t_0} \rho \mathcal{E} & \equiv -\partial_j \rho \mathcal{E} u_j - \partial_j \mathcal{Q}_j^{(0)} - \partial_j u_i \cdot \mathcal{P}_{i,j}^{(0)} + Q_j \\ \partial_{t_n} \rho \mathcal{E} & \equiv -\partial_j \mathcal{Q}_j^{(\mathrm{n})} - \partial_j u_i \cdot \mathcal{P}_{i,j}^{(\mathrm{n})}; \qquad (n > 0) \end{array} \tag{50}$$

With this, the following consistent expansion of ∂_t is obtained[15]:

$$\partial_t = \partial_{t_0} + \varepsilon \partial_{t_1} + \varepsilon^2 \partial_{t_2} + ... \tag{52}$$

3. With defined expansions (36), (45) and (52), the LBE transport equation (24) can be written as[16]:

$$\begin{array}{l} \left[\left(\partial_{t_0} + \varepsilon \partial_{t_1} + \varepsilon^2 \partial_{t_2} + ... \right) + \mathsf{D} \right] \left(f_a^{(0)} + \varepsilon f_a^{(1)} + \varepsilon^2 f_a^{(2)} + ... \right) = \\ = -\frac{1}{\varepsilon \tau} \left[\left(f_a^{(0)} + \varepsilon f_a^{(1)} + \varepsilon^2 f_a^{(2)} + ... \right) - f_a^{\mathrm{eq}} \right] + \frac{a_j}{c_s^2} (e_{a_j} - u_j) f_a^{\mathrm{eq}} \end{array} \tag{53}$$

4. Now, we define $f_a^{(\mathrm{n})}$ *uniquely* by requiring that in eq.(53), the coefficient of each power of ε vanish separately. Thus, the equations to be solved to yield all the

[15] This definition is different from [2] and [14], where the time derivative is expanded as

$$\partial_t = \varepsilon \partial_{t_1} + \varepsilon^2 \partial_{t_2} + ... \tag{51}$$

[16] Let us remind, that $\hat{(\cdot)}$ is omitted.

$f_a^{(\mathrm{n})}$ are

Successive hierarchy of the LBGK equations:

$$
\begin{array}{lcll}
\left(\varepsilon^{-1}\right) & : & f_a^{(0)} & = f_a^{\mathrm{eq}} \\
 & & 0^{th}\text{-order: ``Euler''} & \\
\left(\varepsilon^{0}\right) & : & \partial_{t_0} f_a^{(0)} + \mathsf{D} f_a^{(0)} & = -\frac{f_a^{(1)}}{\tau} + \frac{a_j}{c_s^2}(e_{a_j} - u_j) f_a^{(0)} \\
 & & 1^{st}\text{-order: ``Navier-Stokes''} & \\
\ldots & & \ldots & \\
 & & \text{High-order: ``Burnett'', ``Super-Burnett''} & \\
\ldots & & \ldots & \\
\left(\varepsilon^{k}\right) & : & \partial_{t_0} f_a^{(\mathrm{k})} + \partial_{t_1} f_a^{(\mathrm{k}-1)} + \ldots + \partial_{t_k} f_a^{(0)} + \mathsf{D} f_a^{(\mathrm{k})} & = -\frac{f_a^{(\mathrm{k}+1)}}{\tau} \\
\ldots & & \ldots &
\end{array}
\tag{54}
$$

In the Chapman-Enskog theory for 'continuous' Boltzmann equation, in order to reproduce the Navier-Stokes equations, only the first two approximations $f_a^{(0)}$ and $f_a^{(1)}$ are required[17]. In the next section, we recover and analyze equations of hydrodynamics corresponding to three most commonly used isothermal[18] LBE models.

[17] There exist certain fundamental difficulties when one tries to use truncations of the Chapman-Enskog expansion beyond the Navier-Stokes order $f_a^{(1)}$, ('Burnett-' and 'super-Burnett' equations level). The most significant problem is that any truncation beyond $f_a^{(1)}$ is inconsistent with the Clausius-Duhem inequality, which is often taken as a representation of the second law of thermodynamics [75]. This fact was first noted for compressible gas dynamics by Bobylev [6] and later by Luk'shin [51]. Furthermore, the modifications of Navier-Stokes equations due to Burnett might have been expected to be superior to Navier-Stokes equations itself, under conditions of high Kn numbers. But all present evidence indicates that this is not so; in fact, where the Navier-Stokes equations are themselves perhaps not completely adequate, the higher-order equations may even be inferior. Perhaps the expansion eq.(41) is asymptotic; when the first two terms give a very good approximation, the third may give even better approximation; but when the first two terms do not provide so good approximation, taking another term may make matters worse; this is a known behavior in asymptotic series [21].

[18] Modeling of the 'complete' set of Navier-Stokes and energy equations (with conservation of energy as well as mass and momentum) using the discrete kinetic approach has met significant difficulties. There are three major 'plagues' of the LBE thermohydrodynamics. *First*, the TLBE models employing single-relaxation time are limited to $Pr = \frac{1}{2}$ [2]. *Second*, due to the limited set of the discrete particle velocities utilized in the LBE method, there are severe limitations on allowable variations of temperature and velocity. This hampers the use of the LBE model for simulation of compressible flow and fluids undergoing large temperature variations. *Third*, 'thermal' LBE models are prone to significant numerical instabilities. This is probably related to the fact that 'thermal' LBEs require the 'larger stencil' of discrete velocities, because more constraints on the 'discrete' equilibrium distribution function must be imposed in order to preserve energy conservation and to recover correct macroscopic equations. From this point of view, 'thermal' LBE are somewhat remnant of the higher-order finite difference schemes in 'traditional' CFD, in which the 'large stencil', used to approximate point-to-point solution by high-order polinomials, is prone to oscillations and numerical instabilities [79]. Even though some of these limitations could be alleviated (e.g., [39] [7] [55] [80]), *there is no potential advantage of the 'thermal' LBE approach over a conventional Navier-Stokes solvers for thermal systems and compressible flows* (McNamara et al. [55] [56] and Guangwu et al. [23]). In particular, in [56], the thermal LBE model is compared to the "traditional CFD" finite-difference code, utilizing the MacCormack scheme. It was found, that, in the case of the LBE approach, the running times on the comparable size grids are a factor two greater. Furthermore, the memory requirements are significantly greater; and a numerical stability property is significantly poorer.

2.3.2. Hydrodynamic equations of the isothermal 'ideal fluid' LBGK model

Classical Navier-Stokes equations. The governing equations of the compressible isothermal Newtonian fluid hydrodynamics are

$$\begin{aligned} \partial_t \rho + \partial_j \rho u_j &= 0 \\ \partial_t \rho u_i + \partial_j \rho u_i u_j &= -\partial_i P + \partial_j \mathcal{T}_{i,j} + \rho a_i \end{aligned} \tag{55}$$

where the viscous stress tensor has the following form [4] [48]:

$$\mathcal{T}_{i,j} = \eta \left(\partial_j u_i + \partial_i u_j \right) + \underbrace{\left(\xi - \frac{2}{3}\eta \right)}_{\substack{\text{'Bulk' viscosity,} \\ \lambda}} \partial_k u_k \cdot \delta_{i,j} \tag{56}$$

and η and ξ are the 'first' and the 'second' fluid viscosities. Following Stokes, the 'bulk' and 'second' viscosities are $\lambda = -\frac{2}{3}\eta$ and $\xi = 0$, respectively, [4].

LBGK hydrodynamic equations[19,20]**.** For this 'basic' LBGK model, the pressure tensor is given by

$$\hat{\mathcal{P}}^{(0)}_{i,j} = \hat{\rho}\hat{c}_s^2 \cdot \delta_{i,j} \tag{57}$$

Since the "zeroth-order solution of the LBGK equation", eq.(54), is $\hat{f}_a^{(0)} = \hat{f}_a^{(\mathrm{eq})}$, the momentum flux tensor is $\hat{\Pi}^{(0)}_{i,j} = \hat{\Pi}^{(\mathrm{eq})}_{i,j}$. Thus, the momentum conservation equation (41), which is the "first-order solution of the LBGK equation", is:

$$\partial_t \hat{\rho}\hat{u}_i + \partial_{\hat{j}} \hat{\rho}\hat{u}_i\hat{u}_j = -\partial_i \hat{\rho}\hat{c}_s^2 - \partial_{\hat{j}} \left(\underbrace{\varepsilon \hat{\mathcal{P}}^{(1)}_{i,j}}_{\substack{\text{Viscous stress} \\ \text{tensor,} \\ -\hat{\mathcal{T}}^{\mathrm{LBGK}}_{i,j}}} \right) + \hat{\rho}\hat{a}_i \tag{58}$$

An assumption of the constant temperature would require the following constraint be satisfied:

$$\begin{aligned} \partial_{\hat{j}} \hat{\mathcal{Q}}^{(0)}_j &= -\varepsilon \partial_{\hat{j}} \hat{\rho}\hat{u}_j - \partial_{\hat{j}} \hat{u}_i \cdot \hat{\mathcal{P}}^{(0)}_{i,j} + \hat{Q}_j \\ \partial_{\hat{j}} \hat{\mathcal{Q}}^{(1)}_j &= -\partial_{\hat{j}} \hat{u}_i \cdot \hat{\mathcal{P}}^{(1)}_{i,j} \end{aligned} \tag{59}$$

For this LBGK model, the viscous stress term is (details of the derivation are given in Appendix C):

$$-\partial_{\hat{j}} \left(\varepsilon \hat{\mathcal{P}}^{(1)}_{i,j} \right) = \partial_{\hat{j}} \hat{\mathcal{T}}^{\mathrm{LBGK}}_{i,j} = \partial_{\hat{j}} \left[\hat{\mathcal{T}}_{i,j} \right] + \hat{\mathsf{A}}^{(\mathrm{n.l.d.})}_{i,j} \tag{60}$$

[19] To avoid confusion, in the present section, we will use $\hat{(\cdot)}$ to denote non-dimensional variables.

[20] In the following analysis, it is assumed that the lattice geometry is chosen in such a way so that $\Upsilon^{(4)} = \hat{c}_s^4$.

where $\hat{\mathcal{T}}_{i,j}$ is the non-dimensional Navier-Stokes viscous stress tensor, defined by eq.(56); $\hat{\mathsf{A}}^{(\mathrm{n.l.d.})}_{i,j}$ is a term of the "non-linear[21] deviation" of this LBGK model from the classical Navier-Stokes equations, given by

$$\begin{aligned}\hat{\mathsf{A}}^{(\mathrm{n.l.d.})}_{i,j} \;=\; & \tfrac{1}{\mathsf{Re}\;\hat{c}_s^2}\quad \Big[\partial_{\hat{j}}\left(-2\hat{u}_i\hat{u}_j\hat{u}_k\partial_{\hat{k}}\hat{\rho}\right) - \partial_{\hat{j}}\hat{\rho}\cdot\left(\hat{u}_i\partial_{\hat{k}}\hat{u}_k\hat{u}_j + \hat{u}_j\partial_{\hat{k}}\hat{u}_k\hat{u}_i\right) - \\ & \qquad -\hat{\rho}\partial_{\hat{j}}\left(\hat{u}_i\partial_{\hat{j}}\hat{u}_k\hat{u}_j + \hat{u}_j\partial_{\hat{i}}\hat{u}_k\hat{u}_i\right)\Big] + \\ & + \tfrac{1}{\mathsf{Re}\;\mathsf{Fr}\;\hat{c}_s^4}\;\partial_{\hat{j}}\left(\hat{\rho}\hat{u}_i\hat{u}_j\hat{u}_k\hat{i}_k\right)\end{aligned} \tag{61}$$

where $\mathsf{Re} = \frac{\hat{\rho}}{\hat{\eta}} = \frac{1}{\hat{\nu}}$ and Fr are the Reynolds and Froude numbers, respectively.

Thus, the governing equations of this LBGK model are

$$\begin{aligned}&\partial_{\hat{t}}\hat{\rho} + \partial_{\hat{j}}\hat{\rho}\hat{u}_j = 0 \\ &\underbrace{\partial_{\hat{t}}\hat{\rho}\hat{u}_i + \partial_{\hat{j}}\hat{\rho}\hat{u}_i\hat{u}_j = -\partial_{\hat{i}}\hat{P} + \partial_{\hat{j}}\left[\frac{\hat{\rho}}{\mathsf{Re}}\left(\partial_{\hat{j}}\hat{u}_i + \partial_{\hat{i}}\hat{u}_j\right)\right] + \frac{\hat{\rho}}{\mathsf{Fr}}\hat{i}_i}_{\text{Linear Part} \equiv \text{Navier-Stokes}} + \underbrace{\hat{\mathsf{A}}^{(\mathrm{n.l.d.})}_{i,j}}_{\text{Non-linear deviations}}\end{aligned} \tag{62}$$

where $\hat{i}_i$ is a unit vector specifying the orientation of the external body force.

Now we can immediately see the implications of $\hat{c}_s$, the dimensionless "Internal-Lattice Speed", introduced in eq.(24). In the linear term, it leads to the $\hat{\nu}$ and the Reynolds number that appears in front of the linear part. By appropriate choices of $\hat{c}_s$ and $\hat{\tau}$, flow with any Reynolds number (any viscosity) can be modeled by eq.(62). On the other hand, in the non-linear term, we are left with terms that contain, in addition to Re, $\hat{c}_s^2$ and $\hat{c}_s^4$. Thus, we can make these terms as small as we wish by requiring that $\hat{c}_s$ is chosen so that

$$\left(\mathsf{Re}\;\hat{c}_s^2\right) \gg 1 \quad \text{and} \quad \left(\mathsf{Re}\;\mathsf{Fr}\;\hat{c}_s^4\right) \gg 1 \tag{63}$$

In fact, it turns out that these conditions are automatically satisfied as long as $\hat{c}_s \gg 1$, and the basic stability criterion for integration of the LBE, namely that $\frac{c_s\delta_t}{\delta_x} < 1$ are satisfied. To see this, take N as the number of lattice points in the cross-stream direction ($\mathsf{N} \gg 1$), and suppose we chose $\frac{c_s\delta_t}{\delta_x} = \frac{1}{\sqrt{3}}$. We then have

$$\frac{1}{\mathsf{Re}\;\hat{c}_s^2} = \frac{1}{\sqrt{3}\mathsf{N}\hat{c}_s}$$

from which is seen that the condition $\hat{c}_s \gg 1$ is moderate because $\mathsf{N} \gg 1$. Also, you will note that for inertia flows, $\mathsf{Re} \gg 1$, the condition on $\hat{c}_s \gg 1$ is moderate[22], but for viscous flows, $\mathsf{Re} < 1$, we must obey a stronger condition on $\hat{c}_s \gg 1$, so that $\mathsf{Re}\;\hat{c}_s^2 \gg 1$ and the "non-linear term" is smaller than the inertia "term".

We have verified numerically that indeed, as long as these conditions and $\frac{\Delta\rho}{\rho} \ll 1$ are satisfied, exact solutions can be obtained arbitrarily close in Poisseulle and

[21] The term "non-linear" reflects the fact that the deviation is 'cubic' in velocity, $\sim u_i u_j u_k$.

[22] The smallest term in the Navier-Stokes equations is of order $\frac{1}{\mathsf{Re}}$, thus, the requirement for $\hat{c}_s$ is $\frac{1}{\mathsf{Re}} \gg \frac{1}{\mathsf{Re}\hat{c}_s^2}$

Couette flows, for any values of viscosity (or Reynolds number). Also note that as appropriate for incompressible viscous flows, the pressure level is immaterial. If the pressure drop is specified, it implies a corresponding density drop, through eq.(57), and care must be exercised, because errors will be introduced unless $\frac{\Delta\rho}{\rho}$ remains much less than 1.

Viscosity. The 'first' and the 'second' viscosities are defined as[23]

$$\hat{\eta} = \hat{\tau}\varepsilon\hat{\rho}\hat{c}_s^2 = \underbrace{\frac{\tau\hat{c}_s^2\mathsf{U}_0}{\mathsf{L}}}_{\frac{1}{\mathsf{Re}}}\hat{\rho}; \qquad \hat{\xi} = \frac{2}{3}\hat{\eta} \tag{64}$$

which renders the following definition of the dimensional kinematic viscosity:

$$\nu = \tau c_s^2 \tag{65}$$

In the actual LBE simulations, one employs the following dimensionless relaxation parameter (see eq.(5)):

$$\tau^\star \equiv \frac{\varepsilon\hat{\tau}}{\hat{\delta}_t} = \frac{\tau}{\delta_t} \tag{66}$$

which is typically chosen in the range $\frac{1}{2} < \tau^\star < 3$, where the lower limit is dictated by consideration of the numerical stability of the scheme.

Thus, the kinematic viscosity is[24]

$$\nu = \tau^\star\delta_t c_s^2; \quad \text{or} \quad \underbrace{\nu = \left(\tau^\star - \frac{1}{2}\right)\delta_t c_s^2}_{\text{"stream-and-collide"}} \tag{67}$$

From eq.(67), it is seen that in order to model fluid with specific kinematic viscosity (say, water or air) for a chosen spatial discretization δ_x and relaxation parameter $\tau^\star$, one has to fix time step of the LBE simulation. For example, in the case of the D_2Q_9 "stream-and-collide" scheme with $w_0 = \frac{4}{9}$, time step is

$$\delta_t = \frac{\left(\tau^\star - \frac{1}{2}\right)\delta_x^2}{3\nu}; \quad \hat{\delta}_t = \frac{\left(\tau^\star - \frac{1}{2}\right)\hat{\delta}_x^2\mathsf{Re}}{3} \tag{68}$$

Setting the range of the kinematic viscosity from $10^{-7}\frac{m^2}{s}$ (water) to $10^{-3}\frac{m^2}{s}$ (highly viscous oils), simulation using the space resolution $\delta_x = 1\text{mm}$ and relaxation parameter $\left(\tau^\star - \frac{1}{2}\right) \sim 1$ would require the following range of time step: δ_t varying from $\frac{1}{3}\cdot 10\text{s}$ to $\frac{1}{3}\cdot 10^{-3}\text{s}$. It is interesting to compare these estimates with the "viscous" CFL ("Courant-Friedrichs-Levy") limit of the explicit schemes of

[23] The $\hat{\xi}$ is not Stokesian, $\hat{\xi} \neq 0$. Though, the value of the 'second' viscosity is not important as long as velocity field is close to the 'divergence-free' condition of the incompressible fluid.

[24] In the case of the "stream-and-collide" scheme (see section 4), there is an additional 'numerical' viscosity coefficient absorbed into ν by modifying $\tau^\star \to \left(\tau^\star - \frac{1}{2}\right)$. This coefficient is due to the first-order accuracy of the advection operator, and it would appear if one employs the expansion eq.(35), [76].

the "traditional" CFD, $\delta_t = \mathsf{CFL}_{\mathsf{vis}} \frac{\delta_x^2}{\nu} \sim \mathsf{CFL}_{\mathsf{vis}} \left(10 \div 10^{-3}\right) s$. From this, one can make the following observations. First, the "viscous CFL number" of the LBE is $\mathsf{CFL}_{\mathsf{vis}}{}^{(\mathrm{LBE})} = \left(\tau^\star - \frac{1}{2}\right) \frac{c_s^2}{c^2} = \left.\frac{\tau^\star - \frac{1}{2}}{3}\right|_{D_2Q_9}$. Next, for $\tau^\star > 3.5$, the D_2Q_9 LBE method allows to utilize larger time step than the one admissable for explicit "traditional CFD" schemes, $\mathsf{CFL}_{\mathsf{vis}}{}^{(\mathrm{LBE})} > 1$. However, for small relaxation parameter, $\tau^\star \to \frac{1}{2}$, time step of the LBE becomes too small, $\mathsf{CFL}_{\mathsf{vis}} \ll 1$. This is one of the reasons why the LBE method is inefficient for simulation of high-Re-number flows[25].

Scaling analysis of the non-linear deviations. To estimate the order of the non-linear deviation term, we cast the LBGK hydrodynamic equation (62) into the following dimensional form:

$$
\begin{array}{ccccccc}
\underbrace{\partial_t \rho u_i}_{\left|\begin{array}{c}\sim \frac{\rho_{\mathrm{r}} \mathsf{U}_0{}^2}{\mathsf{L}}(1+\delta\rho_{\mathrm{t}}) \\ \hline \sim 0\,(1+\delta\rho_{\mathrm{t}})\end{array}\right|} & + & \underbrace{\partial_j \rho u_i u_j}_{\left|\begin{array}{c}\sim \frac{\rho_{\mathrm{r}} \mathsf{U}_0{}^2}{\mathsf{L}}(1+\delta\rho_{\mathrm{L}}) \\ \hline \sim 0\,(1+\delta\rho_{\mathrm{L}})\end{array}\right|} & = \partial_i P + & \underbrace{\rho a_i}_{\left|\begin{array}{c}\sim \frac{\rho_{\mathrm{r}} \mathsf{U}_0{}^2}{\mathsf{L}}\frac{1}{\mathsf{Fr}} \\ \hline \sim 0\left(\frac{1}{\mathsf{Fr}}\right)\end{array}\right|} & + \\
\\
+ \underbrace{\partial_j \left[\rho\nu\left(\partial_j u_i + \partial_i u_j\right)\right]}_{\left|\begin{array}{c}\sim \frac{\rho_{\mathrm{r}} \mathsf{U}_0{}^2}{\mathsf{L}}\frac{1+\delta\rho_{\mathrm{L}}}{\mathsf{Re}} \\ \hline \sim 0\left(\frac{1+\delta\rho_{\mathrm{L}}}{\mathsf{Re}}\right)\end{array}\right|} + & & \underbrace{A_{i,j}^{(\mathrm{n.l.d.})}}_{\left|\begin{array}{c}\sim \frac{\rho_{\mathrm{r}} \mathsf{U}_0{}^2}{\mathsf{L}}\frac{(1+\delta\rho_{\mathrm{L}})}{\hat{c}_s^2\ \mathsf{Re}} \\ \hline \sim 0\left(\frac{(1+\delta\rho_{\mathrm{L}})}{\mathsf{Re}\ \hat{c}_s^2}\right)\end{array}\right| \text{ and } \left|\begin{array}{c}\sim \frac{\rho_{\mathrm{r}} \mathsf{U}_0{}^2}{\mathsf{L}}\frac{(1+\delta\rho_{\mathrm{L}})}{\hat{c}_s^4\ \mathsf{Re}\ \mathsf{Fr}} \\ \hline \sim 0\left(\frac{(1+\delta\rho_{\mathrm{L}})}{\hat{c}_s^4\ \mathsf{Re}\ \mathsf{Fr}}\right)\end{array}\right|} & &
\end{array}
\tag{69}
$$

where the Froude numbers is defined as $\mathsf{Fr} \equiv \frac{\mathsf{U}_0^2}{a\mathsf{L}}$; a is an acceleration due to the external body force. The non-dimensional density variations are introduced as $\delta\rho_{\mathrm{L}} \equiv \frac{\Delta_{\mathrm{L}}\rho}{\rho_{\mathrm{r}}}$ and $\delta\rho_{\mathrm{t}} \equiv \frac{\Delta_{\mathrm{t}}\rho}{\rho_{\mathrm{r}}}$, with $\Delta_{\mathrm{L}}\rho$ and $\Delta_{\mathrm{t}}\rho$ being the scales of density variation over a characteristic length scale L, $\partial_i\rho \sim \frac{\Delta_{\mathrm{L}}\rho}{\mathsf{L}}$, and time scale $\mathsf{t}_0 = \frac{\mathsf{L}}{\mathsf{U}_0}$, $\partial_t\rho \sim \frac{\Delta_{\mathrm{t}}\rho}{\mathsf{t}_0}$, respectively. It can be seen that the non-linear deviation term is negligibly small comparing to the Navier-Stokes equation terms under conditions[26] $\hat{c}_s \gg 1$ (or $\Upsilon^{(2)} \gg 1$, see Table 1).

In difference to our derivation, the LBGK hydrodynamic equations available in the literature contain also *linear deviations*. For example, re-arranging the LBGK hydrodynamic equations given in [13] and [63] in a similar way as eq.(69), one can

[25] As seen from eq.(68), in order to increase the Re number for a chosen discretization $\hat{\delta}_x$ and $\hat{\delta}_t$, one needs to decrease the relaxation time $\tau^\star \to \frac{1}{2}$. This causes two problems. First, dimensional time step δ_t decreases according to eq.(68); and, second, the "stream-and-collide" LBE schemes become numerically unstable when $\tau^\star \approx \frac{1}{2}$, [76]. Another alternative for increasing the Re number, keeping δ_t sufficiently large with $\tau^\star$ in the stability region, is to decrease the non-dimensional lattice step $\hat{\delta}_x \sim \frac{1}{\mathsf{N}}$ by increasing the number of computational nodes N. This makes the LBE simulation of high-Re-number flows computationally expensive.

[26] Recently, Qian and Zhou [65] explored a way to eliminate the non-linear term by extending the "lattice stencil" from nine to 17 discrete velocities in 2D case.

obtain the following "linear deviation term":

$$\mathsf{A}_{i,j}^{(\mathrm{l.d.})} = \underbrace{\nu\left[\partial_j\rho\cdot(2\partial_j u_i+\partial_i u_j)+\partial_i\rho\cdot\partial_j u_j+u_i\partial_j^2\rho+u_j\partial_i\partial_j\rho\right]}_{\left|\sim\frac{\rho_r \mathsf{U}_0{}^2}{\mathsf{L}}\frac{\delta\rho_\mathsf{L}}{\mathsf{Re}}\right|}_{\left|\sim 0\left(\frac{\delta\rho_\mathsf{L}}{\mathsf{Re}}\right)\right|} \tag{70}$$

which is negligible in comparison to the Navier-Stokes terms in the limit $\delta\rho_\mathsf{L} \ll 1$.

The following linear and non-linear deviations can be obtained by re-arranging the LBGK hydrodynamic equations of ref. [64]:

$$\mathsf{A}_{i,j}^{(\mathrm{l.d.})} = \underbrace{\nu\partial_j\rho\left(\partial_j u_i+\partial_i u_j\right)}_{\left|\sim\frac{\rho_r \mathsf{U}_0{}^2}{\mathsf{L}}\frac{\delta\rho_\mathsf{L}}{\mathsf{Re}}\right|}_{\left|\sim 0\left(\frac{\delta\rho_\mathsf{L}}{\mathsf{Re}}\right)\right|}; \qquad \underbrace{\mathsf{A}_{i,j}^{(\mathrm{n.l.d.})} = -\nu\partial_j\partial_k\frac{\rho u_i u_j u_k}{c_s^2}}_{\left|\sim\frac{\rho_r \mathsf{U}_0{}^2}{\mathsf{L}}\frac{\delta\rho_\mathsf{L}}{\hat{c}_s^2\,\mathsf{Re}}\right|}_{\left|\sim 0\left(\frac{\delta\rho_\mathsf{L}}{\hat{c}_s^2\,\mathsf{Re}}\right)\right|} \tag{71}$$

Both the linear and non-linear terms are negligible under conditions $\delta\rho_\mathsf{L} \ll 1$ and $\hat{c}_s \gg 1$.

Compressibility effects. It can be seen that the LBE model is not actually incompressible in a "classical" fluid dynamics sense, which requires the velocity field be solenoidal $\nabla\cdot\mathbf{u}=0$ and $\rho = const$. There are always density variations and velocity divergence sources present due to the linearized equation of state $P = c_s^2\rho$ (see eqs.(73) and (74)). The undesirable compressibility effects are minor as long as density variations are small[27,28], $\sim \mathsf{O}(\delta\rho_\mathsf{L})$, $\sim \mathsf{O}(\delta\rho_\mathrm{t})$, $\sim \mathsf{O}\left(\frac{\delta\rho_\mathsf{L}}{\mathsf{Re}}\right)$, and thermodynamic effects are not considered.

[27] There are several LBGK models developed in an attempt to reduce these compressibility effects [15] [30], in which different 'incompressible' techniques are borrowed from the 'traditional' CFD. In particular, He and Luo [30] employed Chorin's "pseudo-compressibility" method [16], in which instead of eq.(38) the following macroscopic 'pressure' equation is introduced:

$$\frac{1}{c_s^2}\partial_t P + \partial_j u_j = 0 \tag{72}$$

Instead of the mass and momentum, the P and $P\mathbf{u}$ are conserved. Eqs.(72) and (58) become a 'target' macroscopic model in "heuristically" building the equilibrium distribution function. In the case of the steady flow, this model completely recovers the 'divergence-free' velocity field. In case of the transient flow, the requirement $\delta\rho_\mathrm{t} \ll 1$ is still necessary to keep divergence sources suppressed.

[28] Another remarkable "incompressible" LBE model is due to Chen and Ohashi [15]. In this model, the incompressibility condition $\nabla\cdot\mathbf{u}$ is regained by applying velocity correction - the idea borrowed from the 'traditional' CFD 'projection' methods [67].

Velocity divergence sources

$$\underbrace{\partial_j u_j}_{\substack{\sim \frac{\mathsf{U}_0}{\mathsf{L}} \\ \sim 0\,(1)}} = \underbrace{\underbrace{-\partial_t \ln \rho}_{\substack{\sim \frac{\mathsf{U}_0}{\mathsf{L}}\delta\rho_{\mathsf{t}} \\ \sim 0\,(\delta\rho_{\mathsf{t}})}} \underbrace{-u_j \partial_j \ln \rho}_{\substack{\sim \frac{\mathsf{U}_0}{\mathsf{L}}\delta\rho_{\mathsf{L}} \\ \sim 0\,(\delta\rho_{\mathsf{L}})}}}_{\text{Compressibility effects (Mass)}} \sim \mathsf{O}\left(\max\left[\delta\rho_{\mathsf{t}}, \delta\rho_{\mathsf{L}}\right]\right) \tag{73}$$

Incompressible Navier-Stokes Part	$\underbrace{\partial_t u_i}_{\substack{\sim \frac{\mathsf{U}_0^2}{\mathsf{L}} \\ \sim 0\,(1)}} + \underbrace{u_j \partial_j u_i}_{\substack{\sim \frac{\mathsf{U}_0^2}{\mathsf{L}} \\ \sim 0\,(1)}} = -\frac{\partial_i P}{\rho} \underbrace{+a_i}_{\substack{\sim \frac{\mathsf{U}_0^2}{\mathsf{L}}\frac{1}{\mathsf{Fr}} \\ \sim 0\left(\frac{1}{\mathsf{Fr}}\right)}} \underbrace{+\partial_j\left[\nu\left(\partial_j u_i + \partial_i u_j\right)\right]}_{\substack{\sim \frac{\mathsf{U}_0^2}{\mathsf{L}}\frac{1}{\mathsf{Re}} \\ \sim 0\left(\frac{1}{\mathsf{Re}}\right)}}$
Deviation from Incompressible Navier-Stokes	$\overbrace{\underbrace{-u_i\partial_t \ln\rho}_{\substack{\sim \frac{\mathsf{U}_0^2}{\mathsf{L}}\delta\rho_{\mathsf{t}} \\ \sim 0\,(\delta\rho_{\mathsf{t}})}} \underbrace{-\frac{u_i \partial_j \rho u_j}{\rho}}_{\sim \frac{\mathsf{U}_0^2}{\mathsf{L}} \max\left[\delta\rho_{\mathsf{t}}, \delta\rho_{\mathsf{L}}\right]} \underbrace{+\nu\left(\partial_j u_i + \partial_i u_j\right)\cdot\partial_j \ln\rho}_{\sim \frac{\mathsf{U}_0^2}{\mathsf{L}}\frac{\delta\rho_{\mathsf{L}}}{\mathsf{Re}}}}^{\text{Compressibility effects (Momentum)}}$ $\overbrace{\underbrace{+\frac{A_{i,j}^{(\text{n.l.d.})}}{\rho}}_{\left\|\frac{\sim \frac{\mathsf{U}_0^2}{\mathsf{L}}\frac{(1+\delta\rho_{\mathsf{L}})}{c_s^2\,\mathsf{Re}}}{\sim \mathsf{O}\left(\frac{(1+\delta\rho_{\mathsf{L}})}{c_s^2\,\mathsf{Re}}\right)}\right\| \text{ and } \left\|\frac{\sim \frac{\mathsf{U}_0^2}{\mathsf{L}}\frac{(1+\delta\rho_{\mathsf{L}})}{c_s^4\mathsf{Re}\,\mathsf{Fr}}}{\sim \mathsf{O}\left(\frac{(1+\delta\rho_{\mathsf{L}})}{c_s^2\,\mathsf{Re}\,\mathsf{Fr}}\right)}\right\|}}^{\text{Non-linear deviation}}$

(74)

Modeling of acoustics. Simulation of the compressible fluid using the isothermal "ideal gas" LBGK model, would require significant computational resources. In particular, in order to adequately represent the sound speed in air ($c_s\,|_{T=300K} = \sqrt{RT} \approx 300\frac{m}{s}$ and $\nu_{\mathsf{air}} \approx 10^{-5}\frac{m^2}{s}$), considered as an ideal gas, a hypothetical simulation would require time step $\delta_t = \frac{\nu}{\left(\tau^\star - \frac{1}{2}\right)c_s^2} \approx 10^{-8}s$, if the D_2Q_9 "stream-and-collide" LBGK scheme is utilized with $\left(\tau^\star - \frac{1}{2}\right) = 10^{-2}$ (probably, the lowest stability limit of this scheme). The correspondent grid size is $\delta_x = \sqrt{3}c_s\delta_t \approx 1\mu m$.

Similar estimates for water[29] ($c_s \approx 1500\frac{m}{s}$ and $\nu_{H_2 0} \approx 10^{-7}\frac{m^2}{s}$) yield $\delta_t \approx 10^{-11}s$ and $\delta_x \approx 10nm$.

2.3.3. Hydrodynamic equations of the isothermal 'free-energy-based' LBGK model for non-ideal fluid

In order to represent complex thermodynamic effects of non-ideal fluids, several "non-ideal fluid" LBGK models have been developed. One of the first successful "non-ideal" LBGK model is due to Swift et al., [77] and [78]. For this model, the pressure tensor is defined using the Cahn-Hilliard's approach for non-equilibrium thermodynamics[30,31] [10]

$$\mathcal{P}_{i,j}^{(0)} = \left[P_0 - \kappa\rho\partial_k^2\rho - \frac{\kappa}{2}\left(\partial_k\rho\right)^2\right]\delta_{i,j} + \kappa\partial_i\rho\cdot\partial_j\rho \tag{75}$$

Thermodynamical pressure P_0 is given by, e.g., van der Waals model, eq.(16). Parameter κ is a measure of the interface free energy. In the case of the flat interface, the coefficient κ is related to the coefficient of surface tension σ through the equation:

$$\kappa = \frac{\sigma}{\int\left(\frac{\partial\rho}{\partial n}\right)^2 dn} \tag{76}$$

where n is a normal-to-interface direction.

So far, no successful implementation of the body force for this model is known, $a_j = 0$. Thus, the governing hydrodynamic equations of this LBGK model written in the "dimensional form" are:

$$\begin{array}{ccccc}
\partial_t\rho & + & \partial_j\rho u_j & = & 0 \\
\underbrace{\partial_t\rho u_i} & + & \underbrace{\partial_j\rho u_i u_j} & = & -\ \underbrace{\partial_i P_0} \\
\overline{\left|\sim\frac{\rho_r \mathsf{U}_0{}^2}{\mathsf{L}}\left(1+\delta\rho_t\right)\right|} & & \overline{\left|\sim\frac{\rho_r \mathsf{U}_0{}^2}{\mathsf{L}}\left(1+\delta\rho_L\right)\right|} & & \overline{\left|\sim\frac{\rho_r \mathsf{U}_0{}^2}{\mathsf{L}}\delta\rho_L\hat{c}_s^2\right|} \\
\overline{\left|\sim 0\left(1+\delta\rho_t\right)\right|} & & \overline{\left|\sim 0(1+\delta\rho_L)\right|} & & \overline{\left|\sim 0\left(\delta\rho_L\hat{c}_s^2\right)\right|}
\end{array}$$

$$+\underbrace{\partial_j\left[\left(\kappa\rho\partial_k^2\rho + \frac{\kappa}{2}\left(\partial_k\rho\right)^2\right)\delta_{i,j} - \kappa\partial_i\rho\cdot\partial_j\rho\right]}_{\overline{\left|\begin{array}{c}\text{'Capillary stress tensor',}\\ \mathsf{K}_{i,j}\sim\frac{\rho_r \mathsf{U}_0{}^2}{\mathsf{L}}\frac{\delta\rho_L\left(1+\delta\rho_L\right)}{\mathsf{We}}\end{array}\right|}} - \partial_j\Big(\underbrace{\rho_r \mathsf{U}_0{}^2\varepsilon\hat{\mathcal{P}}_{i,j}^{(1)}}_{\begin{array}{c}\text{Viscous stress}\\ \text{tensor, } -\mathcal{T}_{i,j}^{\mathrm{LBGK}}\end{array}}\Big) \tag{77}$$

$$\overline{\left|\sim 0\left(\frac{\delta\rho_L\left(1+\delta\rho_L\right)}{\mathsf{We}}\right)\right|}$$

[29] Importantly, water cannot be considered as an "ideal gas" due to the "stiff" pressure-density relation, $P \sim \rho^{7.15}$.

[30] The name 'free-energy-based' is attributed to the model chosen for pressure tensor eq.(75). Strictly speaking, this model is phenomenological, in which the thermodynamic effects are introduced by the *phenomenological equation of state*, but not from the consideration of the kinetic nature of the Lattice Boltzmann method.

[31] In the present section, we use $\hat{(\cdot)}$ to explicitely denote non-dimensional variables.

where the Weber number and density variations are defined as $\mathsf{We} \equiv \frac{\rho_r \mathsf{U}_0{}^2 \mathsf{L}}{\sigma}$, $\delta\rho_{\mathsf{L}} = \frac{\rho_l - \rho_v}{\rho_r}$ and $\delta\rho_t = \frac{\Delta_t \rho}{\rho_r}$, respectively; ρ_l and ρ_v are the saturation density of the liquid and vapor phase under chosen temperature T; and $\Delta_t\rho$ is a scale of the density variation over characteristic time scale $\mathsf{t}_0 \equiv \frac{\mathsf{L}}{\mathsf{U}_0}$. In the scaling analysis of eq.(77), the temporal and spatial derivatives of the density are estimated as $\partial_t \rho \sim \frac{\mathsf{U}_0 \Delta\rho_t}{\mathsf{L}}$, $\partial_i \rho \sim \frac{\rho_l - \rho_v}{\mathsf{L}}$; $\partial_{ij}\rho \sim \frac{\rho_l - \rho_v}{\mathsf{L}^2}$ and $\partial_{ijk}\rho \sim \frac{\rho_l - \rho_v}{\mathsf{L}^3}$. In addition, parameters κ, a and b are scaled as $\kappa \sim \frac{\mathsf{L}\sigma}{\rho_r^2} = \frac{\mathsf{L}^2 \mathsf{U}_0^2}{\rho_r \mathsf{We}}$, $\mathsf{a} \sim \frac{c_s^2}{\rho_r}$ and $\mathsf{b} \sim \frac{1}{\rho_r}$, respectively.

Derivation of the viscous stress tensor $\mathcal{T}_{i,j}^{\mathrm{LBGK}}$ is similar to that one for the "isothermal ideal gas" model and given in appendix C:

$$\partial_j\left(\mathcal{T}_{i,j}^{\mathrm{LBGK}}\right) = \underbrace{\partial_j \mathcal{T}_{i,j}}_{\overline{\left|\sim \frac{\rho_r \mathsf{U}_0{}^2}{\mathsf{L}} \frac{1+\delta\rho_{\mathsf{L}}}{\mathsf{Re}}\right|}} + \mathsf{A}_{i,j}^{(\mathrm{l.d.})} + \underbrace{\mathsf{A}_{i,j}^{(\mathrm{n.l.d.})}}_{\overline{\left|\sim 0\left(\frac{1+\delta\rho_{\mathsf{L}}}{\mathsf{Re}}\right)\right|}} \tag{78}$$

In the analysis of the present section, we assume that the lattice geometry is such, so $\Upsilon^{(4)} = \hat{c}_s^4$. With this, the following viscosities are obtained:

$$\eta = \underbrace{\tau c_s^2}_{\nu}\rho; \quad \xi = \eta\left(\underbrace{\frac{5}{3} + 2\frac{\mathsf{a}\rho}{c_s^2} - \frac{1}{1-\mathsf{b}\rho} - \frac{\rho\mathsf{b}}{(1-\mathsf{b}\rho)^2}}_{\overline{\left|\sim 0(1)\right|}} + \underbrace{\kappa\frac{\partial_l^2\rho}{c_s^2}}_{\overline{\left|\sim 0\left(\frac{\delta\rho_{\mathsf{L}}}{\hat{c}_s^2\mathsf{We}}\right)\right|}}\right) \tag{79}$$

Notably, the second viscosity is non-Stokesian[32]. It is also dependent on the virial coefficients of the equation of state and second gradients of density.

The "linear deviation tensor" is given by the following equation:

[32] For this model, there are strong velocity divergence sources at the interface, making the second viscosity important.

$$
\begin{aligned}
\mathsf{A}_{i,j}^{(\mathrm{l.d.})} = \tfrac{\nu}{c_s^2} \Bigg\{ \partial_j \Bigg[\Bigg(& \underbrace{\left(2\mathsf{a}\rho - \frac{c_s^2}{1-\mathsf{b}\rho} - \frac{\rho c_s^2 \mathsf{b}}{(1-\mathsf{b}\rho)^2}\right) u_k}_{\left|\sim \frac{\rho_r \mathsf{U}_0{}^2}{\mathsf{L}} \frac{\delta\rho_\mathsf{L}}{\mathsf{Re}}\right| \over \left|\sim 0\left(\frac{\delta\rho_\mathsf{L}}{\mathsf{Re}}\right)\right|} \underbrace{+\kappa\left(u_k \partial_l^2 \rho + \partial_{kl}\rho u_l\right)}_{\left|\sim \frac{\rho_r \mathsf{U}_0{}^2}{\mathsf{L}} \frac{\delta\rho_\mathsf{L}}{\hat{c}_s^2 \mathsf{ReWe}}\right| \over \left|\sim 0\left(\frac{\delta\rho_\mathsf{L}}{\hat{c}_s^2 \mathsf{ReWe}}\right)\right|} \Bigg) \partial_k \rho \delta_{i,j} \\
& - \partial_i \rho \left[\underbrace{\kappa \partial_{jk} \rho u_k}_{\left|\sim 0\left(\frac{\delta\rho_\mathsf{L}}{\hat{c}_s^2 \mathsf{ReWe}}\right)\right|} + \underbrace{u_j \left(\frac{c_s^2}{1-\mathsf{b}\rho} + \frac{\rho c_s^2 \mathsf{b}}{(1-\mathsf{b}\rho)^2}\right) - 2\mathsf{a}\rho u_j}_{\left|\sim 0\left(\frac{\delta\rho_\mathsf{L}}{\mathsf{Re}}\right)\right|} \right] - \\
& - \partial_j \rho \left[\underbrace{\kappa \partial_{ik} \rho u_k}_{\left|\sim 0\left(\frac{\delta\rho_\mathsf{L}}{\hat{c}_s^2 \mathsf{ReWe}}\right)\right|} + \underbrace{u_i \left(\frac{c_s^2}{1-\mathsf{b}\rho} + \frac{\rho c_s^2 \mathsf{b}}{(1-\mathsf{b}\rho)^2}\right) - 2\mathsf{a}\rho u_i}_{\left|\sim 0\left(\frac{\delta\rho_\mathsf{L}}{\mathsf{Re}}\right)\right|} \right] \Bigg] \Bigg\}
\end{aligned}
\tag{80}
$$

and the "non-linear deviation tensor" is:

$$
\begin{aligned}
\mathsf{A}_{i,j}^{(\mathrm{n.l.d.})} = & -\tfrac{\eta}{c_s^2} \partial_j \left[u_i \partial_k u_k u_j + u_j \partial_k u_k u_i \right] - \\
& - \underbrace{\frac{\hat{\nu}}{c_s^2} \left\{ \partial_j \left[\partial_k \rho \cdot 2 u_i u_j u_k \right] + \left[u_i \partial_k u_k u_j + u_j \partial_k u_k u_i \right] \cdot \partial_j \rho \right\}}_{\sim \frac{\rho_r \mathsf{U}_0{}^2}{\mathsf{L}} \frac{(1+\delta\rho_\mathsf{L})}{\hat{c}_s^2 \mathsf{Re}} \over \sim 0\left(\frac{(1+\delta\rho_\mathsf{L})}{c_s^2 \mathsf{Re}}\right)}
\end{aligned}
\tag{81}
$$

The linear deviation term includes unphysical capillary terms of order $\sim 0\left(\frac{\delta\rho_\mathsf{L}}{\hat{c}_s^2\ \mathsf{Re}\ \mathsf{We}}\right)$. Comparison of these terms with the capillary stress tensor and Navier-Stokes viscous stress tensor gives

$$
\frac{\mathsf{A}^{(\mathrm{l.d.})}{}_{i,k}}{\mathsf{K}_{i,k}} \sim 0\left(\frac{1}{\hat{c}_s^2 \left(1+\delta\rho_\mathsf{L}\right) \mathsf{Re}}\right)
$$

and

$$\frac{\mathsf{A}^{(\mathrm{l.d.})}{}_{i,k}}{\partial_j \mathcal{T}_{i,j}} \sim \mathsf{O}\left(\frac{\delta\rho_{\mathrm{L}}}{1+\delta\rho_{\mathrm{L}}}\frac{1}{\hat{c}_s^2 \mathsf{We}}\right)$$

which indicates that in order to have the unphysical surface tension suppressed, one has to keep large $\hat{c}_s$.

Furthermore, the "linear deviation term" includes terms of unphysical viscous stresses of the order $\sim \mathsf{O}\left(\frac{1+\delta\rho_{\mathrm{L}}}{\mathsf{Re}}\right)$. Comparison of these "artifacts" with the Navier-Stokes viscous stress tensor:

$$\frac{\mathsf{A}^{(\mathrm{l.d.})}{}_{i,k}}{\partial_j \mathcal{T}_{i,j}} \sim \mathsf{O}\left(\frac{\delta\rho_{\mathrm{L}}}{1+\delta\rho_{\mathrm{L}}}\right)$$

indicates that these unphysical terms cannot be neglected for large density differences $\rho_{\mathrm{l}} - \rho_{\mathrm{v}}$, even for conditions of vanishing Mach number. This is one of the reasons why this LBGK scheme suffers from few unphysical effects, such as Galilean invariance problem [78].

Non-linear deviation. Unphysical viscous stresses due to the non-linear deviation can be suppressed by keeping small Mach numbers,

$$\frac{\mathsf{A}^{(\mathrm{n.l.d.})}{}_{i,k}}{\mathsf{K}_{i,k}} \sim \mathsf{O}\left(\frac{We}{\hat{c}_s^2\delta\rho_{\mathrm{L}}}\right)$$

and

$$\frac{\mathsf{A}^{(\mathrm{n.l.d.})}{}_{i,k}}{\partial_j \mathcal{T}_{i,j}} \sim \mathsf{O}\left(\frac{1}{\hat{c}_s^2}\right)$$

Additional serious methodological drawback of this model is that even though one can introduce the concept of temperature from the consideration of the pressure tensor, it is in conflict with the energy conservation considered in the LBE discrete kinetic theory, eq.(44) - the fact noticed firstly by Luo [50]. That is, one cannot demonstrate that the 'constant-temperature' condition eq.(59) is satisfied. This seems to be a problem for all "isothermal" LBGK models.

2.3.4. Hydrodynamic equations of the isothermal 'HSD' LBGK model for non-ideal fluid

For this model, the pressure tensor and body force are given by

$$\begin{gathered}\mathcal{P}^{(0)}_{i,j} = \rho c_s^2 \cdot \delta_{i,j} \\ F_{i,j} = \rho a_j \delta_{i,j}; \quad a_j = \frac{-\partial_j P^\star + \kappa\rho\partial_j\partial_k^2\rho + \rho g_j}{\rho}\end{gathered} \tag{82}$$

where g_j is an acceleration due to the external body force; and the 'non-ideal' part of the equation of state $P^\star$ is given by, e.g., van der Waals eqs.(15) and (16).

Important methodological difference of this model from the 'free-energy-based' model is the way the 'non-ideal effects' are incorporated. In the 'free-energy-based' approach, the non-ideal equation of state (pressure) is included through the 'momentum flux tensor' constraint imposed on the equilibrium distribution function, eq.(B.1), while in the 'HSD' model, it is incorporated directly through the momentum source term.

With this, the momentum conservation equation written in the "dimensional" form is:

$$\underbrace{\partial_t \rho u_i}_{\left|\begin{array}{c}\sim \frac{\rho_r \mathsf{U}_0{}^2}{\mathsf{L}}(1+\delta\rho_t)\\ \sim 0\,(1+\delta\rho_t)\end{array}\right|} \quad \underbrace{+\partial_j \rho u_i u_j}_{\left|\begin{array}{c}\sim \frac{\rho_r \mathsf{U}_0{}^2}{\mathsf{L}}(1+\delta\rho_L)\\ \sim 0(1+\delta\rho_L)\end{array}\right|} = -\partial_i \underbrace{(\rho c_s^2 + P^\star(\rho))}_{\text{Non-ideal gas pressure}} \underbrace{+\kappa\rho\partial_i\partial_j^2\rho}_{\text{'Capillary stress tensor' } \mathsf{K}_{i,j}}$$

$$\left|\begin{array}{c}\sim \frac{\rho_r \mathsf{U}_0{}^2}{\mathsf{L}}\hat{c}_s^2\delta\rho_L\\ \sim 0\left(\hat{c}_s^2\delta\rho_L\right)\end{array}\right| \qquad \left|\begin{array}{c}\sim \frac{\rho_r \mathsf{U}_0{}^2}{\mathsf{L}}\frac{\delta\rho_L}{\mathsf{We}}\\ \sim 0\left(\frac{\delta\rho_L}{\mathsf{We}}\right)\end{array}\right|$$

$$- \quad \partial_j\Big(\underbrace{\rho_r \mathsf{U}_0^2 \varepsilon \hat{\mathcal{P}}_{i,j}^{(1)}}_{\text{Viscous stress tensor, } -\mathcal{T}_{i,j}^{\mathrm{LBGK}}}\Big) \quad \underbrace{+\rho g_i}_{\left|\begin{array}{c}\sim \frac{\rho_r \mathsf{U}_0{}^2}{\mathsf{L}}\frac{1}{\mathsf{Fr}}\\ \sim 0\left(\frac{1}{\mathsf{Fr}}\right)\end{array}\right|} \tag{83}$$

$$- \quad \underbrace{\partial_j \mathcal{T}_{i,j}}_{\left|\sim 0\left(\frac{1+\delta\rho_L}{\mathsf{Re}}\right)\right|} \quad -\mathsf{A}_{i,j}^{(\mathrm{l.d.})} - \mathsf{A}_{i,j}^{(\mathrm{n.l.d.})}$$

The 'constant-temperature' condition is defined by eq.(59).

The viscous stress tensor $\mathcal{T}_{i,j}^{\mathrm{LBGK}}$ is derived in appendix C. Choosing the lattice with $\Upsilon^{(4)} = \hat{c}_s^4$, the 'first' and the 'second' viscosities are defined by eq.(64). The **"linear deviation"** tensor is:

$$\mathsf{A}_{i,j}^{(\mathrm{l.d.})} = \underbrace{-\frac{\nu}{c_s^2}\left\{\partial_j\left[-\rho\kappa\left[u_i\partial_j^3\rho + u_j\partial_i^3\rho - \left(u_i\partial_j\partial_k^2\rho + u_j\partial_i\partial_k^2\rho\right)\right]\right]\right\}}_{\left|\begin{array}{c}\sim \frac{\rho_r \mathsf{U}_0{}^2}{\mathsf{L}}\frac{\delta\rho_L(1+\delta\rho_L)}{\hat{c}_s^2\mathsf{ReWe}}\\ \sim 0\left(\frac{\delta\rho_L(1+\delta\rho_L)}{\hat{c}_s^2\mathsf{ReWe}}\right)\end{array}\right|} \tag{84}$$

Comparing this unphysical term with capillary and viscous stress tensors:

$$\begin{array}{rcl}\frac{\mathsf{A}_{i,j}^{(\mathrm{l.d.})}}{\mathsf{K}_{i,j}} & \sim & \mathsf{O}\left(\frac{(1+\delta\rho_L)}{\hat{c}_s^2\mathsf{Re}}\right)\\ \frac{\mathsf{A}_{i,j}^{(\mathrm{l.d.})}}{\partial_j\mathcal{T}_{i,j}} & \sim & \mathsf{O}\left(\frac{\delta\rho_L}{\hat{c}_s^2\mathsf{We}}\right)\end{array} \tag{85}$$

indicates that keeping large $\hat{c}_s \gg 1$, this "artifact" can be considered as negligibly small, even for large density ratios $\frac{\rho_l}{\rho_v} \gg 1$, which is significant improvement in comparison to the "free-energy-based" approach.

"Non-linear deviation" tensor is given by the following equation:

$$
\begin{aligned}
\mathsf{A}_{i,j}^{(\mathrm{n.l.d.})} \;=\; -\tfrac{\nu}{c_s^2}\Bigg\{ \partial_j \Bigg[& \underbrace{-\left(2\mathsf{a}\rho + c_s^2 - \frac{c_s^2}{1-\mathsf{b}\rho} - \frac{\rho c_s^2 \mathsf{b}}{(1-\mathsf{b}\rho)^2}\right)\frac{u_i u_j u_k}{c_s^2}\partial_k\rho}_{\overline{\left|\sim \mathsf{O}\left(\frac{\delta\rho_{\mathsf{L}}}{\hat{c}_s^2\mathsf{Re}}\right)\right|}} - \\
& \underbrace{-\rho\kappa\left[\left(\partial_k\partial_l^2\rho\right)\frac{u_i u_j u_k}{c_s^2}\right]}_{\overline{\left|\sim \mathsf{O}\left(\frac{\delta\rho_{\mathsf{L}}(1+\delta\rho_{\mathsf{L}})}{\hat{c}_s^4\mathsf{ReWe}}\right)\right|}} + \underbrace{2u_i u_j u_k\partial_k\rho}_{\overline{\left|\sim \mathsf{O}\left(\frac{\delta\rho_{\mathsf{L}}}{\hat{c}_s^2\mathsf{Re}}\right)\right|}} - \\
& \partial_j\rho\left[\underbrace{\frac{u_i u_j u_k}{c_s^2}g_k}_{\overline{\left|\sim \mathsf{O}\left(\frac{\delta\rho_{\mathsf{L}}}{\hat{c}_s^4\mathsf{ReFr}}\right)\right|}} \underbrace{-u_i\partial_k u_j u_k - u_j\partial_k u_i u_k}_{\overline{\left|\sim \mathsf{O}\left(\frac{\delta\rho_{\mathsf{L}}}{\hat{c}_s^2\mathsf{Re}}\right)\right|}}\right] \Bigg\} \\
& +\tfrac{\eta}{c_s^2}\partial_j\left[\underbrace{\frac{u_i u_j u_k g_k}{c_s^2}}_{\overline{\left|\sim \mathsf{O}\left(\frac{1}{\hat{c}_s^4\mathsf{ReFr}}\right)\right|}} \underbrace{-u_i\partial_k u_j u_k - u_j\partial_k u_i u_k}_{\overline{\left|\sim \mathsf{O}\left(\frac{1}{\hat{c}_s^2\mathsf{Re}}\right)\right|}}\right]
\end{aligned}
\tag{86}
$$

and includes terms of order $\sim \mathsf{O}\left(\frac{1+\delta\rho_{\mathsf{L}}+\delta\rho_{\mathsf{L}}^2}{\hat{c}_s^4\mathsf{ReWe}}\right)$ and $\sim \mathsf{O}\left(\frac{1+\delta\rho_{\mathsf{L}}}{\hat{c}_s^2\mathsf{Re}}\right)$, which allows to make this unphysical term be suppressed by keeping the limit $\hat{c}_s \gg 1$.

3. MODELING OF INHOMOGENEOUS FLUIDS AND FLUID-FLUID INTERFACES

Modeling of gas-gas, gas-liquid, liquid-liquid flows and interfacial phenomena is one of the most difficult area in the computational fluid dynamics. The major challenge is to properly describe *the physics of the interface evolution* (transport, breakup and coalescence). The difficulty is mainly related to the fact that the concepts of the continuum mechanics - the ground of the "traditional" computational fluid dynamics - are not applicable across the interfaces, where the drastical change

of material properties occurs. Considering interfaces, one naturally and intuitively thinks in terms of molecules of different kind, interacting over very short distance across the interfaces. Thus, intuitively, the models operating with the concept of particles and molecules should have methodological advantage over methods of the 'continuum mechanics'. Since the lattice Boltzmann equation method is the *particle method*, it is oftenly seen to be superior comparing to the 'traditional CFD' methods [71] [72] [73] [74] [77] [78] [84]. In the present section, we would like to discuss the existing LBE models for multiphase flows, trying to address the question whether, why and when the LBE approach is advantageous for simulation of the interfacial phenomena. It is important to realize that the computational modeling of multiphase flows is not open for 'purism'. That is, there are no 'universal models' able to perfectly work under any flow conditions. One has to be aware of the limitations and advantages of the approach chosen, since every one has its own domain of applicability. Thus, we start with our classification of the modern computational methods for fluid-fluid multiphase flows, which would enable us to properly appreciate the perspectives of the discrete kinetic approach.

Based on the underlying physical concept of the interface, the modern CFD methods for fluid-fluid multiphase flows can be separated into three groups[33]:

1. **"Free-boundary Approaches", FBA**. In the classical fluid mechanics, the interface between two immiscible fluids is modeled as a free boundary which evolves in time. It is assumed that fluid dynamics equations of motion hold in each fluid. These equations are supplemented by boundary conditions at the free surface, involving the physical properties of the interface[34]. The formulation results in a free-boundary problem (Lamb, 1932 [46], Batchelor, 1967 [5], etc.). It is assumed that physical quantities, such as e.g. density, are discontinuous across the interface. Physical processes such as e.g. capillarity occurring at the interface, are represented by boundary ("jump") conditions imposed there. Representative example of computational methods involving "free-boundary formulation" is the *boundary element/boundary integral method*, (BE/BIM) ([70] [86]).

2. **"Physical-Diffuse-Interface Approaches", PDIA** [3]. The approaches of this group are based on the Poisson's (1831) [61] Maxwell's (1876) [53] and Gibbs's (1876) [20] concept of the interface as a rapid and smooth transition of physical properties between the bulk fluid values. This idea was further developed by Rayleigh (1892) [66] and van der Waals (1893) [83] with their "gradient theories for the interface" based on thermodynamic principles, and Korteweg (1901) [45], who proposed a constitutive law for the capillary stress tensor in terms of the density and its spatial gradients. Examples of the "PDIA" CFD models are the "second-gradient theory", "phase-field" and "Model H" [37]. These models are based on the "continuum mechanics methodology", in which transport equations for macroscopic variables are constructed, introducing phenomenological physical

[33] We will discuss only the 'direct numerical simulation' (DNS) methods (i.e. those which resolve interface), putting aside 'effective field' (EF) methods , which employ statistically-/, time- or spatially-averaged equations for multiphase systems ([19] [41]).

[34] This approach originates from probably the earliest concept of fluid-fluid interfaces: Young, Laplace and Gauss, in the early part of the 1800's, considered the interface between two fluids as a surface of zero thickness endowed with physical properties such as surface tension.

models for interfacial dynamics through the effective forcing terms in the momentum equations ("capillary stress tensors", "free-energy" concept, Cahn-Hilliard's approach, etc.) and additional evolution equations for "order" parameters. The "PDIA" CFD models are quite successful in describing many different interfacial phenomena, including studies of critical point scaling laws [37], capillary waves [27], moving contact lines [68], droplets and nucleation [18], droplet breakup [42] and spinoidal decomposition [24] (see for review [3]).

3. **"Numerical-Diffuse-Interface Approaches", NDIA**. The methods of this group involve a numerical method to "capture" or "track" interface (e.g., the transport equation for "volume-of-fluid", VOF [36], the level set equation, LSA, [69] or "front-tracking" technique by Tryggvason [82]). Then, the interface region is numerically smeared-out over few computational nodes, allowing numerically smooth transition of fluid properties (i.e., density and viscosity); and, in this "numerical diffuse interface" region, the capillary effects are included as "body forces", which in effect mimic the Korteweg's capillary stress tensor.

To discuss the LBE method for multiphase flows, we have chosen three most successful and popular LBE models: the 'Shan-Chen' ('SC') model; the 'free-energy-based' model; and the 'He-Shan-Doolen' ('HSD') model. The other multiphase LBE models are due to Gunsteinsten at al. [25] and Luo [50].

3.1. Interparticle interaction potential model of Shan and Chen ("SC")

One of the first and probably most used "multiphase LBE" model is due to Shan and Chen [71] [72] [73] [74]. In this model, after each time step, an additional momentum forcing term is explicitly added to the velocity field:

$$\mathbf{u}'(\mathbf{x},t) = \mathbf{u}(\mathbf{x},t) + \vec{\Gamma}(\mathbf{x},t) \qquad \text{where} \tag{87}$$
$$\vec{\Gamma}(\mathbf{x},t) = -\frac{\tau}{\rho}\psi(\mathbf{x})\sum_{a}^{b}\mathcal{G}_a\psi(\mathbf{x}+\mathbf{e}_a)\mathbf{e}_a$$

where ψ is a "potential" function and $\mathcal{G}$ is a "strength" of interparticle interaction. The 'corrected' velocity $\mathbf{u}'$ is employed in the equilibrium distribution function, given by eq.(B.9). By introducing an additional forcing term, this model *effectively mimics* the intermolecular interactions.

One can avoid the step eq.(87) by directly substituting $\mathbf{u}'$ into the equilibrium distribution function eq.(B.9). Effectively, this means addition of the following "correction" term to the equilibrium distribution function:

$$f_a^{\mathrm{eq}} = f_a^{\mathrm{eq}} + \delta f_a^{\star}, \quad a = 0,..,b \tag{88}$$
$$\delta f_0^{\star} = \left[\frac{1-w_0}{\Upsilon^{(2)}} - \frac{\Upsilon^{(2)}}{\Upsilon^{(4)}}\right]\cdot\left[\Gamma_i u_i + \frac{\Gamma_i^2}{2\rho}\right] \quad \text{and}$$
$$\delta f_{a\neq 0}^{\star} = w_a\left[\frac{e_{a_i}\Gamma_i - u_i\Gamma_i - \Gamma_i^2/(2\rho)}{\Upsilon^{(2)}} + \frac{e_{a_i}e_{a_j}}{2\Upsilon^{(4)}}\left\{\Gamma_i u_j + \Gamma_j u_i + \frac{\Gamma_i\Gamma_j}{\rho}\right\}\right]$$

The forcing term $\vec{\Gamma}$ in eq.(87) corresponds to the following non-local potential function

$$\mathcal{V}(\mathbf{x},\mathbf{x}') = \mathcal{G}(\mathbf{x},\mathbf{x}')\ \psi(\mathbf{x})\ \psi(\mathbf{x}') \tag{89}$$

Notably, for this model, the momentum is not conserved locally[35]. Thus, there is always spurious velocity present close to the interface[36].

The 'SC' LBE method has been quite successful in simulation of several fundamental interfacial phenomena, such as Laplace law for static droplets/bubbles and oscillation of a capillary wave (see for review [13]).

There are few limitations of the 'SC' model, which have to be overcome in order to make it competitive approach for multiphase flows. The first serious problem is that one cannot introduce temperature which is consistent with the thermodynamical model. It is possible to show that the 'SC' model has the following equation of state [72]:

$$P = c_s^2\rho + \underbrace{\frac{\mathsf{b}c^2\mathcal{G}}{2\mathsf{D}}\psi^2(\rho)}_{P^\star} \tag{90}$$

where $\mathsf{b}=24$ and $\mathsf{D}=2$ for a D_2Q_9 lattice. Suppose we would like to study fluid with the 'non-ideal' part of the equation of state P^*. In order to reproduce this equation of state, the following ψ function must be utilized:

$$\psi(\rho) = \sqrt{\frac{2\mathsf{D}P^\star}{\mathsf{b}c^2\mathcal{G}}};\quad P^\star = P - c_s^2\rho \tag{91}$$

It is possible to show (see [72]), that, for this model, the Maxwell's "equal-area" reconstruction is possible only for one special form of the potential function, $\psi = \psi_0\exp(-\rho_0/\rho)$, where ψ_0 and ρ_0 are arbitrary constants. This makes this model, in general, thermodynamically inconsistent. The role of temperature in this model is effectively taken by the strength of the interparticle interactions $\mathcal{G}$. By varying $\mathcal{G}$, one could construct $(\mathcal{G}-\rho)$-diagram, which mimics the $(T-\rho)$-diagram.

The next problem is related to the way this model represents capillary effects, which can be quantified by the coefficient of surface tension σ. It can be shown [72], that for the 'SC' model, in the case of the flat interface, the coefficient of surface tension can be calculated from the following equation:

$$\sigma = \frac{c^2}{\mathsf{D}+2}\int_{-\infty}^{+\infty}\sqrt{P^\star}\cdot\frac{d^2\sqrt{P^\star}}{dn^2}dn \tag{92}$$

where n is a direction normal to the interface. This means that σ is coupled to the equation of state through P^* and there is no freedom to vary it.

Another limitation is related to the ability of representing different viscosities in different phases, which is important for modeling of real fluids. In most LBE

[35] However, it is possible to show that the total momentum, in the whole computational domain, is conserved [72].

[36] If one defines macroscopic velocity as $\mathbf{u}'$, the interfacial spurious velocity is reduced.

simulations of multiphase flows, it is assumed that all phases or components of the modeled multiphase system have the same kinematic (ν) and "second" ($\frac{\xi}{\rho}$) viscosities, defined by the relaxation time[37] τ and lattice geometry, eq.(64).

In terms of our classification of the CFD methods for fluid-fluid multiphase flows, the 'SC' model is close to the "physical-diffuse-interface" methods. Similar to the 'PDIA' methods, there is no need to "track" or "capture" interface position, since the "phase separation" and "interface sharpening" mechanisms are provided by the physical model for momentum forcing term $\vec{\Gamma}$. Effectively, $\vec{\Gamma}$ plays the role of both the Korteweg's capillary stress tensor and the "non-ideal" part of the equation of state P^*. Similarly to the 'PDIA', the 'SC' method builds the interface physical model based on the continuum variable ρ: $\vec{\Gamma} = \mathcal{F}(\psi = f(\rho))$. There is no direct use of the one-particle probability distribution function, f_a - the major distiquishable feature of the LBE method. So far, there is no clear idea how to make use of f_a for better representation/interpretation of physical phenomena at the interface.

3.2. "Free-energy-based" model by Swift et al.

Another successful LBE model for fluid-fluid multiphase flow is due to Swift et al. [77]. For one-component fluid, this model is introduced in section 2.3.3. Multi-component versions of the model are developed in [78] and [47]. The general idea is to incorporate phenomenological models of interface dynamics, such as Cahn-Hilliard approach and Ginzburg-Landau model, using the concepts of free-energy functional; and to utilize the discrete kinetic approach as a vehicle for coupling with complex-fluid hydrodynamics. The method belongs to the class of the 'physical-diffuse-interface' approaches.

The major advantage of this method over the 'SC' LBE method is that thermodynamical model of complex fluid is properly formulated, based on the physical principles of quasilocal thermodynamics for multi-component fluids in thermodynamic equilibrium at a fixed temperature. In addition, since the model admits local momentum conservation, interfacial spurious velocity is practically eliminated [57].

The free-energy-based LBE approach has been successfully applied to study several physical phenomena in binary and ternary fluids, such as flow patterns in lamellar fluids subjected to shear flow [22]; effect of shear on droplet phase in binary mixtures [84]; spontaneous emulsification of droplet phase in ternary fluid, which mimics the oil-water-surfactant systems [47]; etc.

The major drawback of this approach is that the model suffers from unphysical Galilean invariance effects, coming from the 'non-Navier-Stokes' terms, which appear at the level of the Chapman-Enskog analysis of the discrete Boltzmann equation (see, e.g. section 2.3.3). There are few promising studies, in which these unphysical effects are reduced [38].

Another problem of the free-energy-based LBE approach is that, similarly to the 'SC' model, it actually does not utilize the 'particle' nature of the discrete kinetic approach. That is, the same phenomenological models of quasilocal equilibrium isothermal thermodynamics can also be introduced in the computational methods which directly solve for transport equations for macroscopic variables ("traditional"

[37] One possible way to vary viscosity is to introduce spatially-variable relaxation time, which allows to have different viscosity in 'bulk' regions of different fluids [52].

CFD methods). These are the 'PDIA' methods - see for review [3]. Moreover, using the "traditional CFD" approaches, most of the severe problems of the LBE-based hydrodynamics of complex fluid (inability to represent heat transfer and energy conservation, unphysical terms for the momentum conservation law, stability problem for large density ratios) might be surpassed without significant challenge.

3.3. He, Shan and Doolen ("HSD") model

This model has been recently developed [31] as a revision of the 'SC' model. In difference to the 'SC' model, the 'HSD' model is not heuristic, but has a solid ground in the kinetic theory of dense gases, section 2.1. The intermolecular interactions are coming not from the imposed artificial rules, but from the approximation of the Enskog's extension of the Boltzmann equation. As a result, several limitations of the 'SC' model have been eliminated. In particular, the 'HSD' approach is flexible in implementation of the thermodynamical model, with the "consistent" temperature concept, admitting the correct Maxwell's "equal-area" reconstruction procedure. Furthermore, the capillary effects are modeled by the explicit implementation of the "density gradient model", $\kappa\nabla\nabla^2\rho$, eq.(15), allowing flexibility in variation of the coefficient of surface tension by varying the parameter κ.

There are few limitations of the model, which have yet to be overcome. The most serious one is that this model cannot be acceptable for modeling of phase transition, until the heat transfer phenomena are properly represented. Currently, the 'HSD' model does not describe energy transport, eq.(44). This seems to be a problem for all LBE models of multiphase flows.

The next limitation is related to the numerical instability, associated with the 'stiffness' of the collision operator, when the 'complex fluid' effects are introduced through the 'forcing' term, eq.(15). These stability problems might be alleviated by providing 'robust' numerical schemes for advection and collision operators, like those discussed in section 4 and ref. [81].

Another way to improve stability of the 'HSD' model has been explored in [32]. In this study, two probability distribution functions are utilized. The first one is used to "capture" incompressible fluid's pressure and velocity fields, using the "pseudo-compressibility" concept ([30] and [16]). Another discrete probability distribution function i_a is introduced with the sole purpose to "capture" the interface. After each time step, the "index" function $\phi = \sum_a i_a$ is re-constructed, allowing to enforce a smooth transition of densities and viscosities at the "numerically smeared" interface:

$$\begin{array}{l} \rho\left(\phi\right) = \rho_1 + \frac{\phi-\phi_1}{\phi_2-\phi_1}\left(\rho_2-\rho_1\right) \\ \nu\left(\phi\right) = \nu_1 + \frac{\phi-\phi_1}{\phi_2-\phi_1}\left(\nu_2-\nu_1\right) \end{array} \tag{93}$$

where ρ_1, ρ_2, ν_1 and ν_1 are the densities and kinematic viscosities of two modeled fluids; and ϕ_1, ϕ_2 are the minimum and maximum values of the 'index' function.

With this, this version of the 'HSD' model is close in spirit to the "front capturing" methods of the 'NDIA', where ϕ effectively plays the role of the 'volume-of-fluid' or the 'level set' functions. In [32], this model has been used to simulate Rayleigh-Taylor instability. The results of the simulation are comparable with those obtained by the "traditional" CFD approaches, using the "VOF" and Tryggvason's

"front-tracking" methods.

Summarizing, the LBE methods for fluid-fluid multiphase flows are able to reproduce several basic interfacial phenomena, such as spinoidal decomposition in binary fluids, oscillation of a capillary wave, Rayleigh-Taylor instability, etc., with the results comparable to those obtained by the methods of the "traditional" CFD. From another side, the currently existing multiphase LBE methods are not able to beneficially utilize the 'kinetic theory origin' of the method. That is, in order to simulate the interfacial phenomena, all currently existing LBE models practically employ the same techniques, as those used in the "traditional" CFD: *i.e.*, intermolecular interactions are practically implemented through the phenomenological thermodynamical models - equations of state; and the capillary effects are introduced by utilizing the "density gradient" approaches.

4. NUMERICAL TREATMENT: IMPLEMENTATION, EFFICIENCY AND PERSPECTIVES

Eq.(24) is a system of b PDE Hamilton-Jacobi equations, consisting of an "advection part", $\mathcal{A}(f_a)$ and a "collision part", $\Omega(f_a)$:

$$\underbrace{\frac{\partial f_a}{\partial t} + \frac{\delta_{x_a}}{\delta_t}\frac{\partial f_a}{\partial x_a}}_{\mathcal{A}(f_a)} = \frac{\Omega_a(f_a)}{\delta_t} \tag{94}$$

where the collision operator is $\Omega_a \equiv -\frac{f_a - f_a^{(\mathrm{eq})}}{\tau^\star}$.

The simplest scheme for discretization of each of these equations involves the first-order-accurate implicit forward differencing for an advection,

$$\mathcal{A}(f_a) = \frac{f_a^{(n+1)} - f_a^{(n)}}{\delta_t} + \frac{\delta_a}{\delta_t}\frac{f_{a+1}^{(n+1)} - f_a^{(n)}}{\delta_a}$$

where δ_a is a grid step in the"a^{th}" direction; and the first-order-accurate explicit Euler discretization for a collision, $\Omega_a^{(n)}$ [76] . This results in the "basic" two-step "stream-and-collide" LBE algorithm.

"Stream-and-Collide Algorithm":

- Collision:
  - Flow macroscopic conserved variables are calculated using eq.(32).
  - Equilibrium distribution functions are determined, using eqs.(B.2)-(B.10).
  - 'Ready-to-advect' distribution functions are computed for each lattice direction, at each site:

$$f_a(\mathbf{x} + \mathbf{e}_a\delta_t, t + \delta_t) = f_a(\mathbf{x}, t) + \Omega_a(\mathbf{x}, t); \qquad a = 0, ..., b \tag{95}$$

  - Finally, if necessary (depending on the boundary conditions employed), the r.h.s. side of eq.(95) is modified for boundary nodes.
- Advection. After collision, advection takes place. Particle populations are streamed in the directions of corresponding discrete velocities, towards the neighbor lattice nodes.

One can introduce more elaborate schemes as follows.

4.1. Discretization of the advection operator

Let's consider general three-point finite-difference formula for discretization of the transport partial differential equation (94), at the point i in the "a^{th}" direction of the particle's motion:

$$f_{a,i}^{n+1} = \mathsf{a}_i f_{a,i-1}^{\diamondsuit} + \mathsf{b}_i f_{a,i}^{\diamondsuit} + \mathsf{c}_i f_{a,i+1}^{\diamondsuit} + \Omega_{a,i}^{\diamondsuit} \tag{96}$$

where the upper indices are used to denote the level of implicity: $\diamondsuit = n$ (explicit), $\diamondsuit = n + 1/2$ (semi-implicit), and $\diamondsuit = n + 1$ (implicit). Eq.(96) can be written in the following conservative form, [59]:

$$\begin{aligned} f_{a,i}^{n+1} = f_{a,i}^{n} - \tfrac{1}{2}\Big[\mathrm{CFL}_{i+\frac{1}{2}}(f_{a,i+1}^{\diamondsuit} + f_{a,i}^{\diamondsuit}) - \mathrm{CFL}_{i-\frac{1}{2}}(f_{a,i}^{\diamondsuit} + f_{a,i-1}^{\diamondsuit})\Big] + \\ + \Big[\nu_{i+\frac{1}{2}}^{(\mathsf{n.d.})}(f_{a,i+1}^{\diamondsuit} - f_{a,i}^{\diamondsuit}) - \nu_{i-\frac{1}{2}}^{(\mathsf{n.d.})}(f_{a,i}^{\diamondsuit} - f_{a,i-1}^{\diamondsuit})\Big] + \Omega_{a,i}^{\diamondsuit} \end{aligned} \tag{97}$$

where $\nu_{i\pm\frac{1}{2}}^{(\mathsf{n.d.})}$ are the dimensionless coefficients of numerical diffusion, and

$$\begin{aligned} \mathsf{a}_i &\equiv \nu_{i-\frac{1}{2}}^{(\mathsf{n.d.})} + \tfrac{1}{2}\mathrm{CFL}_{i-\frac{1}{2}} \\ \mathsf{b}_i &\equiv 1 - \tfrac{1}{2}\mathrm{CFL}_{i+\frac{1}{2}} + \tfrac{1}{2}\mathrm{CFL}_{i-\frac{1}{2}} - \nu_{i+\frac{1}{2}}^{(\mathsf{n.d.})} - \nu_{i-\frac{1}{2}}^{(\mathsf{n.d.})} \\ \mathsf{c}_i &\equiv \nu_{i+\frac{1}{2}}^{(\mathsf{n.d.})} - \tfrac{1}{2}\mathrm{CFL}_{i+\frac{1}{2}} \end{aligned} \tag{98}$$

Application of eqs.(96)-(98) to the 'stream-and-collide' equation (95) gives $\nu^{(\mathsf{n.d.})} = 1/2$, [76]. This numerical diffusion can be directly compensated for by modifying the relaxation parameter from $\tau^\star$ to $\tau^\star - 1/2$.

Note, that for a "stream-and-collide" scheme, the "Courant, Friedrichs, and Lewy" number for advection is $\mathsf{CFL} = \frac{e_a \delta_t}{\Delta x_a} \equiv 1$. The use of the CFL=1 is quite restrictive, especially in the case of strong non-linearity of the collision operator. The following 'predictor-corrector' algorithm has been introduced in [57], allowing to alleviate this problem.

"Multifractional stepping procedure (MFN)":

Time step from n to $n+1$ is divided on $2N$ sub-steps (fractions). The downwind/upwind difference are employed for an advection term, at each odd/even sub-step:

$$\begin{aligned} f_{a,i}^{(2m+1)} &= f_{a,i}^{(2m)} + \frac{f_{a,i}^{(2m)} - f_{a,i+1}^{(2m)}}{2N} + \frac{\Omega_{a,i}^{\diamondsuit}}{2N} \\ f_{a,i}^{(2m+2)} &= f_{a,i}^{(2m+1)} + \frac{f_{a,i-1}^{(2m+1)} - f_{a,i}^{(2m+1)}}{2N} + \frac{\Omega_{a,i}^{\diamondsuit}}{2N}, \qquad m = 0, ..., 2N \end{aligned} \tag{99}$$

With this scheme, the CFL number can be varied arbitrarily, CFL=$\frac{1}{2N}$. In the case of $N = 1$, this is exactly the explicit MacCormack scheme [59]. Furthermore, for each couple of sub-steps, we have central differencing for both time and space. Therefore, this scheme is of second order accuracy. Applying eqs.(96)-(98), the coefficient of the numerical diffusion is $\nu^{(\mathrm{n.d.})} = -\frac{1}{4N}$ for odd sub-steps, and

$\nu^{(\mathrm{n.d.})} = +\frac{1}{4N}$ for even sub-steps. Thus, in total, the coefficient of the numerical diffusion is zero.

The other algorithms for discretization of the LBE's advection operator are given in [81] ("TVD/AC" scheme) and [55] ("Lax-Wendroff" scheme). It is shown that these schemes are able to alleviate the LBE stability problems, which are especially acute in the case of the simulation of multiphase and thermal flows ([57] [81] and [55]).

4.2. Discretization of the collision operator

'Stream-and-collide' LBE numerical scheme employs explicit Euler method for a collision operator. In the case of $\omega = \frac{1}{\tau^*} \to 2$, and in the case of the strong non-linearity of the collision operator, this scheme fails to produce stable solution [76] [57]. Notice, that the LBE equations (96)

$$\frac{\mathcal{A}(f_a)}{\omega} \equiv \underbrace{D_\omega f_a = \mathcal{K}} \equiv f_a^{\mathrm{eq}} - f_a \tag{100}$$

are stiff differential equations in ω: $f_a \sim e^{\sim\omega}$. This means, that the errors grow exponentially.

There are several numerical schemes recommended for the solution of stiff differential equations (see for review [59]). One obvious way to reduce error growth, without iterative procedures, is to employ high-order explicit Runge-Kutta methods. Applying these approaches to the LBE equations, the following procedure could be utilized:

"Runge-Kutta Schemes":

- *Collision stage.*

  ♣ **Euler method (E),** $O(\omega)$**:**

  1. Calculate macroscopic variables, $[u_i, \rho, P_{ij}]^n = \mathsf{M}^n(f_a^n)$;
  2. Calculate equilibrium distribution function $f_a^{\mathrm{eq,n}}$ and the collision operator: $\mathcal{K}^\diamondsuit \equiv \frac{\Omega_a^\diamondsuit}{\omega} = f_a^{\mathrm{eq,n}} - f_a^n$.

  ♣ **Improved Euler method (IE),** $O(\omega^2)$**:**

  1. Predictor:
     * Calculate macroscopic variables, $[u_i, \rho, P_{ij}]^\diamondsuit = \mathsf{M}^\diamondsuit(f_a^n)$;
     * Calculate equilibrium distribution function $f_a^{\mathrm{eq,n}}$ and the collision operator: $\mathcal{K}^\diamondsuit = \mathcal{K}^n = f_a^{\mathrm{eq,n}} - f_a^n$.
     * Advance on ω: $f_a^\diamondsuit = f_a^n + \omega\mathcal{K}^\diamondsuit$;
  2. Corrector:
     * Calculate macroscopic variables, $[u_i, \rho, P_{ij}]^\diamondsuit = \mathsf{M}^\diamondsuit(f_a^\diamondsuit)$;
     * Calculate equilibrium distribution function $f_a^{\mathrm{eq},\diamondsuit}$ and a new collision operator: $\mathcal{K}^\diamondsuit = f_a^{\mathrm{eq},\diamondsuit} - f_a^\diamondsuit$.
     * Calculate the final collision term: $\mathcal{K}^\diamondsuit \equiv \frac{\Omega_a^\diamondsuit}{\omega\delta_t} = \frac{\mathcal{K}^n + \mathcal{K}^\diamondsuit}{2}$.

- *Advection stage:* employ one of the advection numerical schemes, $\mathcal{A}(f_a^n \to f_a^{n+1}) = \omega\mathcal{K}^\diamondsuit$, discussed above.

Similarly, one can develop algorithms for other high-order Runge-Kutta schemes. Unfortunately, all Runge-Kutta schemes do not guarantee stability for stiff equations. Therefore, the following *implicit trapezoidal method (IT)* is recommended in [57].

"Implicit Trapezoidal method (IT)":

$$D_\omega f_a = \frac{\mathcal{K}^n + \mathcal{K}^{n+1}}{2} \tag{101}$$

1. *Collision stage*

   (i) $\mathcal{K}^{(m=0)} = \mathcal{K}^n$ [Euler];

   (ii) Iteration loop, $m = m + 1$:

   - $\mathcal{K}^{(m)} = \frac{\mathcal{K}^n + \mathcal{K}^{(m-1)}}{2}$;
   - Relaxation (if needed): $\mathcal{K}^{(m)} = r \cdot \mathcal{K}^{(m)} + (1 - r) \cdot \mathcal{K}^{(m-1)}$; r - is a relaxation parameter;
   - Advection: $\mathcal{A}\left(f_a^n \to f_a^{(m)}\right)$. Get new $f_a^{(m)}$.
   - New macroscopic variables: $[u_i, \rho, P_{ij}]^{(m)} = \mathsf{M}^{(m)}(f_a^{(m)})$;
   - New equilibrium distribution function $f_a^{\star,(m)}$ from $[u_i, \rho, P_{ij}]^{(m)}$.
   - New collision operator: $\mathcal{K}^{(m)} = f_a^{\star,(m)} - f_a^{(m)}$.
   - Convergence test: $\left|\frac{\mathcal{K}^{(m)} - \mathcal{K}^{(m-1)}}{\rho^{(m)}}\right| \leq \varepsilon_c$; ε_c is a 'target' accuracy.
   - Repeat, if not converged.

2. *Advection stage:* $\mathcal{A}(f_a^n \to f_a^{n+1}) = \omega \mathcal{K}^{(m)}$.

This scheme is known to be A-stable (absolute stability in the entire left half-plane, [59]) from the Von Neumann linear stability analysis. Also, it is a second-order accurate scheme, $O(\omega^2)$. However, the 'IT' scheme requires the iterative procedure. Fortunately, the iterations converge rapidly, especially when the 'MFN' scheme is imployed for an advection. Moreover, the more fractions N employed, the faster the convergence [57].

In [57] the 'IT' scheme is applied to the free-energy-based LBE method for non-ideal fluid. It is found that it can significantly improve stability for high-surface-tension and high-density-ratio non-ideal fluids.

4.3. LBE as a solver of Navier-Stokes equations: place, efficiency and perspectives

Looking back at the fundamental principles and aspects of the practical implementation of the LBE method, it is clear that, currently, the fact that the LBE method operates with particle probability distribution function does not give any real advantage in better representation of molecular interactions. Thus, currently existing LBE methods are actually not truly able to "capture" some physical phenomena, which are 'out-of-reach' for 'traditional' CFD methods. In practice, the LBE method is basically used as an alternative mean to solve the Navier-Stokes equations, while the effects of the molecular interactions are represented by the phenomenological models - equations of state - the same approach which is utilized in the 'PDIA' methods of the "traditional CFD". There is also no clear evidence that

the LBE approach is more efficient 'Navier-Stokes solver', than the "traditional" CFD methods. In what follows, we will discuss 'pros' and 'cons' of the LBE method as a 'Navier-Stokes solver', in terms of its simplicity, efficiency and capability for efficient parallelization.

Simplicity. One argument in favor of the LBE method is its simplicity in implementation. Many researchers may find the LBE codes easier to handle, than the "traditional" CFD Navier-Stokes solvers. This is probably a true for a simplest 'stream-and-collide' LBE algorithm with bounceback boundary conditions. Surely, this scheme is much simpler to "code" than the best methods of the "traditional" CFD, which involve algorithms for a solution of Poisson equation; sophisticated Riemann solvers to handle hyperbolic terms; using unstructured grids to handle complex geometry; etc. However, from our experience with both the "traditional CFD" and the "discrete kinetic" approaches, we found that actually there is no significant simplification in using the LBE methodology, if we limit ourselves to the methods of the *comparable* capacity. That is, the direct counterparts of the LBE are the "compressible flow methods for incompressible flows", such as, e.g. widely used Chorin's pseudocompressibility approach for incompressible flow. These methods also do not require Poisson equation solvers, and are quite simple for implementation on regular mesh. Direct counterpart of the LBE's bounce-back boundary conditions is, probably, the method of fictitious ('ghost') cells, with polygonal representation of the complex-geometry boundaries - the simplest approach widely used in many "traditional" CFD N.-S. solvers.

Simplicity of the LBE approach significantly deteriorates, however, when more 'advanced' features are being implemented, such as, e.g., non-uniform and body-fitted lattices; adaptive lattice; high-order-accurate boundary condition treatment; more sophisticated numerical algorithms for advection/collision needed to improve stability; 'finite-volume' LBEs; etc. (see for review [13]). These capabilities are the must for any competitive Navier-Stokes solver, for industrial applications.

Efficiency. Computational efficiency advantages of the 'isothermal' LBE approach is a subject of discussion in several studies. In particular, in [12], the three-dimensional LBE algorithm is reported to be 2.5 times faster than the pseudo-spectral method for incompressible flow, for low-Reynolds-number conditions.

Comparison of the LBE model with "traditional" CFD incompressible finite-volume (FVM) "projection" method (Patankar's and Spalding's SIMPLE algorithm [60]) using the advanced multigrid technique on block-structured grids has been recently performed by Berndorf et al. [9]. As a test-case for a comparison, a channel flow with obstacles has been chosen. The results of calculations indicate that when the number of obstacles is small, the FVM is more efficient than the LBE. This is a direct "penalty" for explicitness of the method, requiring to keep small time step in order to limit compressibility effects by small-Mach-number condition. However, as geometrical complexity of the flow increased, the efficiency of the multigrid[38] Poisson solver is reduced, and, therefore, a break-even point between the multigrid FVM and the LBE exists, where, at certain complexity of the geometry, the LBE method becomes more efficient than the finite volume approach.

[38] Multigrid is currently the best available algorithm for solution of system of algebraic equations.

The advantage of the LBE method for 'large-grid, complex-geometry' configurations is seems to be due to the *explicitness* of the LBE algorithm, which does not involve solution of the Poisson equation. The efficiency of the best available (multigrid) algorithms deteriorate with increase of flow geometrical complexity.

Currently, there is no available direct comparison of the LBE method with the 'pseudocompressible methods' of the "traditional" CFD. Those methods might be as fast and as efficient, as the LBE approach, for massive calculations with complex-geometry configurations, considering the fact that significantly smaller number of governing equations are needed to be solved[39] and smaller number of variables needed to be stored.

The LBE approach, however, might still be superior for *low-*Re*-number flows*, since there is practically no large-viscosity-related numerical stability limitations, which dwindle time step in explicit finite-difference schemes of the "traditional" CFD, $\delta_t \leq \frac{\delta_x^2}{\nu}$ (see discussion in section 2.3.2).

Parallelization. The best criterium to evaluate the method's efficiency in parallelization is *scalability* - the ratio of the computational time spent for the same computational task, by increasing the number of processors involved. We approach parallelization of the LBE algorithm by subdividing the computational domain on $\mathcal{N}$ subdomains, corresponding to $\mathcal{N}$ processors available; solving for each subdomain on separate processor; and connecting the processors in a network using MPI [57]. This is one of the most popular CFD strategy for parallelization [58]. Comparing scalability of the LBE method with scalability of the 'traditional' CFD finite-difference code for compressible fluid dynamics, we have found no significant advantage of either approaches. Depending on the implementation, optimization and the size of the problem considered, scalabilities of both methods are within the range 1.7 - 1.9. There is though some disadvantage of the LBE method, because of the more complex stencil involved, and, thus, the network for connection of processors is more sophisticated. Thus, in two dimensions, each processor, instead of four neighbors of the "traditional" CFD finite-difference code[40], the D_2Q_9 LBE code requires eight neighbors[41]. More sophisticated processor-network is required in three dimensions, fig.1b. Closely related to this is the amount of information to be 'exchanged' at the end of each time step. In the case of the LBE's D_2Q_9 scheme, symbolically, 9×8 float variables are being sent/received, corresponding to nine PPDFs, f_a, and eight neighbor-processors. For the finite-difference code, 3×12 variables must be sent/received, corresponding to three conserved variables

[39] Comparing to the LBE, instead of solving in the most "optimistic" case (D_2Q_6) six explicit equations for f_a ($a = 1, .., 6$), one has to deal with 3 explicit macroscopic equations for $\mathbf{W} = (\rho; \rho u; \rho v)$. This "score" ("3:6") is much worse in 3D, where for the lattice with minimum possible discrete velocities D_3Q_{14} the count is "4:14". For the case of the thermal LBGK models, the minimum number of discrete velocities in 2D is 16 [14], thus, the count is "4:16". In 3D, one needs 40 discrete velocities to recover the correct macroscopic equations, elevating the "score" to "5:40" (see also discussion in [56]). If one attempts to model multicomponent fluids, one has to introduce PPDF for each component, drastically increasing the number of explicit equations solved and the memory storage requirements.

[40] We utilize the high-order-accurate ($WENO_5$ [43]) conservative finite-difference characteristic-based approach [58] [26].

[41] Processors are also connected in 'diagonal' directions, fig.1a.

$(\rho; u; v)$ and [4 'neighbor-processors' $\times$ 3 layers of the finite-difference stencil[42]]. Note, that the scalability of the 'domain decomposition' strategy for parallelization depends on the amount of information sent/received during each 'exchange' stage; and the amount of the computational work to be undertaken by each independent processor. From this perspective, the LBE approach is not advantageous.

5. CONCLUDING REMARKS

The Lattice Boltzmann Equation method is an alternative *approximate scheme* for description of hydrodynamics. As a derivative of the kinetic theory of dilute gases, the domain of the method's validity and applicability corresponds to that of the Boltzmann equation theory: i.e. *hydrodynamics of dilute monoatomic (ideal) gases*. The method is shown to be an effective and reasonably accurate scheme for discretization of the continuous Boltzmann equation, in the limit of *uniform isothermal gases under vanishing Mach number conditions*.

The method belongs to the class of the "compressible CFD methods for simulation of incompressible flows" ("pseudocompressible" methods) and share advantages, disadvantages and limitations of this class of the computational fluid dynamics. This includes the simplicity and explicitness of the algorithm, which requires no solution of the Poisson equation; the restrictive simulation time step in order to maintain the low-Mach-number limit; the artificial compressibility effects, $\nabla \cdot \mathbf{u} = u_j \partial_j \ln \rho - \partial_t \ln \rho \neq 0$, originating from both the linearized equation of state $P_{\mathrm{t/d}} = c_s^2 \rho$ and the discretization errors; and the inability to properly describe thermodynamics and acoustic effects. Similarly to the "pseudocompressible" methods of the "traditional CFD", the LBE approach is efficient in parallelization and *suitable for massive computation of incompressible flows in complex geometry configurations*, such as flow in porous media, particulate and suspension multiphase flows. The LBE method might be more advantageous under *low-*Re*-number* conditions. Thus, this area can be considered as the most perspective direction of the LBE method application.

Extension of the LBE method to nonuniform (non-ideal) gases, and more generally to fluid-fluid multiphase flows, is realized either heuristically (by applying certain rules which "mimic" complex-fluid behaviour); or based on the Enskog's extension of the Boltzmann's theory to dense gases, with incorporation of the phenomenological models of quasilocal equilibrium constant-temperature thermodynamics; and using the LBE methodology to couple the later one to the hydrodynamics of complex fluid. The "complex-fluid" framework of the LBE method is able to reproduce several multiphase flow phenomena with the results, comparable to the methods of the "traditional CFD". There are few challenging problems, which have yet to be overcome in order to demonstrate the LBE scheme as a compatitive and perspective methodology, comparing to the "traditional CFD" approach of direct solution of the conservation equations of continuum mechanics. These include the modeling of heat transfer and energy transport; elimination of excessive numerical discretization errors and robustness and numerical stability under wide range of flow conditions and multiphase flow properties.

[42] 'Size' of the stencil for WENO_5 scheme is 3 [43].

Acknowledgement: The collaboration of D.Joseph was limited to the part of this paper dealing with homogeneous (single-phase) flows (Chapters 1 and 2).

REFERENCES

1. Aidun, C.K., Lu, Y., and Ding, E.-J., Direct Analysis of Particulate Suspensions with Inertia using the Discrete Boltzmann Equation, *J. Fluid Mech.*, **373**, 287-311.
2. Alexander, F.J., Chen, S., and Sterling, J.D., Lattice Boltzmann Thermohydrodynamics, *Physical Review E*, **47** (4), R2249-R2252.
3. Andersen, D.M., McFadden, G.B., and Wheeler, A.A., Diffuse-Interface in Fluid Mechanics, *Annual Review of Fluid Mechanics*, **30**, 139-165, 1998.
4. Aris, R., *Vectors, Tensors, and the Basic Equations of Fluid Mechanics*, Prentice-Hall, Inc., Englewood Cliffs, N.J., 1962.
5. Batchelor., *An Introduction to Fluid Dynamics*, Cambridge: Cambridge University Press, 1967.
6. Bobylev, A.V., The Chapman-Enskog and Grad methods for Solving the Boltzmann Equation, *Sov. Phys. Dokl.*, **27**, 1982.
7. Boghosian, B.M., and Coveney, P.V., Inverse Chapman-Enskog Derivation of the Thermohydrodynamic Lattice-BGK Model for the Ideal Gas, *International Journal of Modern Physics C*, **9** (8), 1231-1245, 1998.
8. Boltzmann, L., Weitere Studien über das Wärmegleichgewicht unter Gasmoleculen, *Wien Ber.*, **66**, 275, 1872.
9. Bernsdorf, J., Durst, F., and Schäfer, A., Comparison of Cellular Automata and Finite Volume Techniques for Simulation of Incompressible Flows in Complex Geometries, *Int. J. for Numer. Meth. Fluids*, **29**, 251-264, 1999.
10. Cahn, J. W., and Hilliard, J. E., *J. Chem. Phys.*, **28**, 258 (1958).
11. Chapmann, S., and Cowling, T.G., The Mathematical Theory of Non-Uniform Gases, *Cambridge University Press*, 1970.
12. Chen, S., Wang, Z., Shan, X., and Doolen, G.D., Lattice Boltzmann Computational Fluid Dynamics in Three Dimensions, *Journal of Statistical Physics*, **68** (3/4), 379-400.
13. Chen, S., and Doolen, G. D., Lattice Boltzmann Method for Fluid Flows, *Annu. Rev. Fluid Mech.*, **30** (4), 329-364.
14. Chen, Y., Ohashi, H., and Akiyama, M., Thermal Lattice Bhatnagar-Gross-Krook Model Without Nonlinear Deviations in Macrodynamic Equations, *Physical Review E*, **50** (4), 2776-2783.
15. Chen, Y., and Ohashi, H., Lattice-BGK Methods for Simulating Incompressible Fluid Flows, *International Journal of Modern Physics C*, **8** (4), 793-803.
16. Chorin, A.J., A Numerical Method for Solving Incompressible Viscous Flow Problems, *Journal of Computational Physics*, **2**, 12, 1967.
17. Clague, D.S., Kandhai, B.D., Zhang, R., and Sloot, P.M.A., Hydraulic Permiability of (un)bounded Fibrous Media using the Lattice Boltzmann Method, *Physical Review E*, **61** (1), 616-625.
18. Dell'Isola, F., Gouin, H., and Seppecher, P., Radius and Surface Tension of Microscopic Bubbles be Second Gradient Theory, *C. R. Acad. Sci. Paris*, **320**, 211-216.
19. Drew, D.A., Passman, S.L., Theory of Multicomponent Fluids, *Applied Mathematical Sciences 135*, Springer, 1999.
20. Gibbs, J.W., On the equilibrium of heterogeneous substances, *Trans. Conn. Acad.*, 3:108-248, 3:343-524, 1878. Reprinted in *The Scientific Papers of J. Willard Gibbs*, pp.55-371. London: Longmans, Green, and Co, 1906.
21. Goldstein, S., Burgers, J.M., Lectures on Fluid Mechanics, *Interscience Publishers, Ltd., London*, 1957.
22. Gonnella, G., Orlandini, E., and Yeomans, J.M., Lattice-Boltzmann Simulation of Complex Fluids, *International Journal of Modern Physics*, **8** (4), 783-792.
23. Guangwu, Y., Yaosong, C., and Shouxin, H., Simple Lattice Boltzmann Model for Simulating Flows with Shock Wave, *Physical Review E*, January 1999, **59** (1), 454-459.

24. Gurtin, M.E., Polignone, D., and Vinals, J., Two-Phase Binary Fluids and Immiscible Fluids Described by an Order Parameter, *Mathematical Models and Methods in Applied Sciences*, **6**, 815 (1996).

25. Gustensen, A.K., Rothman, D.H., Zaleski, S., and Zanetti, G., Lattice Boltzmann Model of Immiscible Fluids, *Phys. Rev. A.*, **43**, 4320-4327 (1991).

26. Fedkiw, R., Merriman, B., Donat, R., and Osher, S., The Penultimate Scheme for Systems of Conservation Laws: Finite Difference ENO with Marquina's Flux Splitting, *Progress in Numerical Solutions of Partial Differential Equations*, Arcachon, France, edited by M. Hafez, July 1998.

27. Felderhof, B.U., Dynamics of the diffuse gas-liquid interface near the critical point, *Physica*, **48** (1970), 541-560.

28. Frisch, U., Hasslacher, B., and Pomeau, Y., Lattice gas Cellular Automata for the Navier-Stokes equations, *Phys. Rev. Lett.*, **56** (1986), 1505.

29. Harris, S., An Introduction to the Theory of the Boltzmann Equation, *Holt, Rinehart and Winston*, New York, 1971.

30. He, X., and Luo, L. -S., Lattice Boltzmann Model for the Incompressible Navier-Stokes Equation, *Journal of Statistical Physics*, **88** (3/4), 1997, 927-944.

31. He, X., Shan, X., and Doolen, G., Discrete Boltzmann equation model for nonideal gases, *Physical Review Letters*, January 1998, **57** (1), R13-R16.

32. He, X., Chen,S., and Zhang, R., A Lattice Boltzmann Scheme for Incompressible Multiphase Flow and Its Application in Simulation of Rayleigh-Taylor Instability, *Journal of Computational Physics*, **152**, 642-663 (1999).

33. He, X., and Luo, L. -S., *A priori* Derivation of the Lattice Boltzmann Equation, *Physical Review E*, June 1997, **55** (6), 6811-6817.

34. He, X., and Luo, L. -S., Theory of the Lattice Boltzmann: From the Boltzmann Equation to the Lattice Boltzmann Equation, *Physical Review E*, December 1997, **56** (6), 6811-6817.

35. He, X., *Private communication.*

36. Hirt, C.W., Nichols, B.D., Volume of Fluid (VOF) methods for the dynamics of free boundaries, *Journal of Computational Physics*, **39**, 201-225.

37. Hohenberg, B.I., and Halperin, P.C., Theory of Dynamic Critical Phenomena, *Reviews of Modern Physics*, **49**(3), 435-479 (1977).

38. Holdych, D.J., Rovas, D., Geogiadis, J.G., and Buckius, R.O., An improved Hydrodynamic Formulation for Multiphase Flow Lattice Boltzmann Models, *International Journal of Modern Physics C*, **9**(8), 1393, (1998).

39. Huang, J., Xu, F., Vallieres, Feng, D.H., Qian, Y.-H., Fryxell, B., and Strayer, M.R., A Thermal LBGK Model for Large Density and Temperature Differences, *International Journal of Modern Physics C*, **8** (4), 827-841, 1997.

40. Huang, K., Statistical Mechanics, *John Wiley & Sons, Inc.*, 1963.

41. Ishii, M., Thermo-Fluid Dynamic Theory of Two-Phase Flow, *Direction des Etudes et Recherches d'Electricité de France*, 1975.

42. Jacqmin, D., An Energy Approach to the Continuum Surface Tension Method, *AIAA 96-0858*, In *Proceedings of the 34th Aerospace Sciences Meeting and Exhibit.* Reno: American Institute of Aeronautics and Astronautics.

43. Jiang, G.S., and Shu, C.-W., Efficient Implementation of Weighted ENO Schemes, *Journal of Computational Physics*, **126**, 202-228, 1996.

44. Koga, T., Introduction to Kinetic Theory Stochastic Processes in Gaseous Systems, *Pergamon Press*, 1970.

45. Korteweg, D.J., Sur la forme que prennent les équations du mouvements des fluides si l'on tient compte des forces capillaires causées par des variations de densité considérables mais continues et sur la théorie de la capillarité dans l'hypothése d'une variation continue de la densité, *Arch. Néerl. Sci. Exactes Nat. Ser.*, II 6, 1-24, 1901.

46. Lamb, H., *"Hydrodynamics"*, Cambridge: Cambridge University Press, 1932.

47. Lamura, A., Gonnella, G., and Yeomans, J.M., A Lattice Boltzmann Model of Ternary Fluid Mixtures, *Europhysics Letters*, 1 February 1999, **99** (3), 314-320.

48. Landau, L. D., and Lifschitz, E. M., *Theoretical Physics, v.VI, "Hydrodynamics"*, Chapter II.15, In Russian, Nauka, Forth Edition, 1988, Moscow.

49. Liboff, R.L., Introduction to the Theory of Kinetic Equations, *John Wiley & Sons, Inc.*, 1969.

50. Luo, L.- S., Unified Theory of Lattice Boltzmann Models for Nonideal Gases, *Physical Review Letters*, 24 August 1998, **81** (8), 1618-1621.

51. Luk'shin, A.V., Hydrodynamical Limit for the Boltzmann Equation and its Different Analogs, in *Numerical Methods in Mathematical Physics*, Moscow State University, Moscow (1986), 61-91.

52. Martys, N.S., and Chen, H., Simulation of Multicomponent Fluids in Complex Three-Dimensional Geometries by the Lattice Boltzmann Method, *Phys. Rev. E*, **53**, (1996), 743-750.

53. Maxwell, J.C., Capillary Action. In *Encyclopaedia Britannica*, (9^{th} edition). Reprinted in *The Scientific Papers of James Clerk Maxwell*, **2**, pp.541-591. New York: Dover, 1952.

54. McNamara, G.R. and Zanetti, G., Use of the Boltzmann Equation to Simulate Lattice-Gas Automata, *Phys. Rev. Lett.*, **61**, Number 20, (1988), 2332.

55. McNamara, G.R., Garcia, A.L., and Alder, B.J., Stabilization of Thermal Lattice Boltzmann Models, *Journal of Statistical Physics*, **81**, Number 1/2, (1995), 395-408.

56. McNamara, G.R., Garcia, A.L., and Alder, B.J., A Hydrodynamically Correct Thermal Lattice Boltzmann Model, *Journal of Statistical Physics*, **87**, Number 5/6, (1997), 395-408.

57. Nourgaliev, R.R., Dinh, T.N., Hattori, S., and Sehgal, B.R., Free-Energy-Based Lattice Boltzmann Model of Phase Transitions in an Isothermal Non-Ideal Fluid, CD-ROM Proceedings of *The Ninth International Topical Meeting on Nuclear Reactor Thermal Hydraulics (NURETH-9)*, San Francisco, October 3-8, 1999.

58. Nourgaliev, R.R., Dinh, T.A., Dalal, D.C., Dinh, T.N., and Theofanous, T.G., MuSiC: Multiscale Simulation Code. "Modeling of Complex Fluid-Fluid and Fluid-Solid Interactions using the Level Set and 'Ghost Fluid' Methodology. Single- and Multiphase Compressible Flows", UCSB-CRSS Research Report, November 20, 2000, 209p.

59. Oran, E. S., and Boris, J. P., Numerical Simulation of Reactive Flow, *Elsevier Science Publishing Co., Inc.*, New York-Amsterdam-London, 1987.

60. Patankar, S.V., and Spalding, D.B., A Calculation Procedure for Heat, Mass and Momentum Transfer in Three-Dimensional Parabolic Flows, *Int. J. Heat Mass Transf.*, **15**, 1787-1806, 1972.

61. Poisson, S.D., *Nouvelle Théorie de l'action capillaire*, Paris: Bachelier, 1831.

62. Qi, D., Lattice-Boltzmann Simulations of Particles in Non-Zero-Reynolds-Number Flows, *J. Fluid Mech.*, **385** , 41, 1999.

63. Qian, Y. H., D'Humiéres, D., and Lallemand, P., Lattice BGK Models for Navier-Stokes Equation, *Europhysics Letters*, **17** (6), 479-484.

64. Qian, Y. H., and Orszag, S.A., Lattice BGK Models for the Navier-Stokes Equation: Nonlinear Deviation in Compressible Regimes, *Europhys. Lett.*, **21**(3), 255-259, 1993.

65. Qian, Y. H., and Zhou, Y., Complete Galilean-Invariant Lattice BGK Models for the Navier-Stokes Equation, *NASA/CR-1998-208701*, ICASE Report No.98-38, August 1998.

66. Lord Rayleigh, On the theory of surface forces. - II. Compressible fluids. *Phil. Mag.*, **33**, pp.209-220, 1892.

67. Rider, W. J. , Approximate Projections Methods for Incompressible Flow: Implementation, Variants and Robustness, *Technical Report LA-UR-2000*, Los Alamos National Laboratory, 1994. Available on World Wide Web at http://www.c3.lanl.gov/cic3/publications/main.html.

68. Seppecher, P., Moving Contact Lines in the Cahn-Hilliard Theory, *Int. J. Engng. Sci*, **34** (9), 977-992, 1996.

69. Sethian, J.A., Level Set Methods and Fast Marching Methods, *Cambridge University Press*, 1999.

70. Schulkes, R.M.S.M, The Evolution and Bifurcation of a Pendant Drop, *J. Fluid Mech.*, **278**, 83, 1994.

71. Shan, X. and Chen, H., Lattice Boltzmann Model for Simulating Flows with Multiple Phases and Components, *Physical Review E*, March 1993, **47** (3), 1815-1819.

72. Shan, X. and Chen, H., Simulation of Nonideal Gases and Liquid-Gas Phase Transitions by the Lattice Boltzmann Equation, *Physical Review E*, April 1994, **49** (4), 2941-2948.

73. Shan, X. and Doolen, G., Multicomponent Lattice-Boltzmann Model with Interparticle Interactions, *Journal of Statistical Physics*, **81** (1/2), 379-393.

74. Shan, X. and Doolen, G., Diffusion in a Multicomponent Lattice Boltzmann Equation Model, *Physical Review E*, October 1996, **54** (4), 3614-3620.

75. Slemrod, M., Constitutive Relations for Monoatomic Gases Based on a Generalized Rational Approximation to the Sum of the Chapman-Enskog Expansion, *Arch. Rational Mech. Anal.*, **150**, 1-22, 1999.

76. Sterling, J.D., and Chen, S., Stability Analysis of Lattice Boltzmann Methods, *Journal of Computational Physics*, **123**, 196-206, 1996.

77. Swift, M. R., Osborn, W. R. and Yeomans, J. M., Lattice Boltzmann Simulations of Nonideal Fluid, *Physical Review E*, November 1996, **54** (5), 5041-5052.

78. Swift, M. R., Orlandini, E., Osborn, W. R. and Yeomans, J. M., Lattice Boltzmann Simulations of Liquid-Gas and Binary Fluid Systems, *Physical Review Letters*, 31 July 1995, **75** (5), 830-833.

79. Succi, S., Lattice Boltzmann equation: Failure or success? *PHYSICA A*, **240**(1-2), 221-228, June 1, 1997.

80. Sun, C., Adaptive Lattice Boltzmann Model for Compressible Flows: Viscous and Conductive Properties, *Physical Review E*, March 2000, **61** (3), 2645-2653.

81. Teng, S. L., Chen, Y., and Ohashi, H., Lattice Boltzmann Simulation of Multiphase Fluid Flows through the Total Variation Diminishing with Artificial Compression Scheme, *Int. J. of Heat and Fluid Flow*, **21**, 112-121, 2000.

82. Unverdi, S.O., Tryggvason, G., A Front-Tracking Method for Viscous, Incompressible, Multi-Fluid Flows, *Journal of Computational Physics*, **100**, 25-37, 1992.

83. van der Waals, Verhandel. Konink. Akad. Weten. Amsterdam (Sect. 1), vol. 1, No. 8 (Dutch). Transl. J.S. Rowlinson, 1979, Translation of J.D. van der Waals' "The thermodynamic theory of capillarity under the hypothesis of a continuous density variation", *J. Stat. Phys.*, **20**, 197-244.

84. Wagner, A.J., and Yeomans, J.M., Effect of Shear on Droplets in a Binary Mixture, *International Journal of Modern Physics C*, **8** (4), 773-782.

85. Wolfram, S., Cellular Automation Fluids 1: Basic Theory, *Journal of Statistical Physics*, **45** (3/4), 471-526.

86. Zhang, D.F., Stone, H.A., Drop formation in viscous flows at a vertical capillary tube, *Phys. Fluids*, **9**, 2234, 1997.

APPENDIX A

Lattice geometry and symmetry

Consider the lattice composed of r sublattices in $\mathcal{D}$ dimensions. Each sublattice has weight w_r, which are chosen to satisfy certain symmetry requirements. In total, the lattice has $a = 0, .., b$ links, $\mathbf{e}_a$.

The most important properties of the lattice are related to the symmetries of the tensors:

$$\mathcal{N}^n_{i_1 i_2 \ldots i_n} = \sum_a w(|\mathbf{e}_a|^2)(\mathbf{e}_a)_{i_1} \ldots (\mathbf{e}_a)_{i_n} \tag{A.1}$$

which are determined from the choice of the basic lattice directions $\mathbf{e}_a$.

The basic condition for standard hydrodynamic behaviour is that tensors $\mathcal{N}^{(n)}$ for $n \leq 4$ should be isotropic [85]. Isotropic tensors $\mathcal{N}^{(n)}$, obtained with sets of b vectors $\mathbf{e}_a$ composing r sublattices in $\mathcal{D}$ space dimensions, must take the form

$$\begin{cases} \mathcal{N}^{(2n+1)} & = 0 \\ \mathcal{N}^{(2n)} & = \Upsilon^{(2n)} \Delta^{(2n)} \end{cases} \tag{A.2}$$

where

$$\begin{cases} \Delta^{(2)}_{i,j} & = \delta_{i,j} \\ \Delta^{(4)}_{i,j,k,l} & = \delta_{i,j}\delta_{kl} + \delta_{ik}\delta_{jl} + \delta_{il}\delta_{jk} \\ \Delta^{(2n)}_{i_1 i_2 \ldots i_{2n}} & = \sum_{j=2}^{2n} \delta_{i_1 i_j} \Delta^{(2n-2)}_{i_2 \ldots i_{j-1} i_{j+1} \ldots i_{2n}} \end{cases} \tag{A.3}$$

Coefficients $\Upsilon^{(2n)}$ in eq.(A.2) are dependent on the specific lattice geometry, and are given in Table 1 for the most commonly used lattices.

APPENDIX B

Equilibrium distribution function

To fit into the Chapman-Enskog procedure (section 2.3.1), the equilibrium distribution function should satisfy the following constraints:

$$\begin{array}{lll} \sum_{a=0}^{b} f_a^{\mathrm{eq}} & = \rho & \text{'Mass conservation'} \\ \sum_{a=0}^{b} f_a^{\mathrm{eq}} e_{a_i} & = \rho u_i & \text{'Momentum conservation'} \\ \underbrace{\sum_{a=0}^{b} f_a^{\mathrm{eq}} e_{a_i} e_{a_j}}_{\Pi^{\mathrm{eq}}_{i,j}} & = P_{i,j} + \rho u_i u_j & \text{'Momentum flux tensor'} \\ \underbrace{\sum_{a=0}^{b} f_a^{\mathrm{eq}} e_{a_i} e_{a_j} e_{a_k}}_{\mathcal{D}^{\mathrm{eq}}_{i,j,k}} & = \mathcal{M}(u_i\delta_{jk} + u_j\delta_{ik} + u_k\delta_{i,j}) & \text{'Constitutive physics'} \end{array} \tag{B.1}$$

where $\mathcal{M}$ and $P_{i,j}$ are the coefficient related to the fluid viscosity and the pressure tensor, respectively.

TABLE 1

Symmetry characteristics of the most commonly used lattices.

Lattice	*Order of symmetry*	r	w_a [b,c]	$\Upsilon^{(2)}$ [d,e]	$\Upsilon^{(4)}$	$\mathbf{e}_a/c$,
D_2Q_7	4^{th}	2	$w_0 = var = \{\frac{1}{2}\}$ $w_{a\neq 0} = \frac{1-w_0}{6}$	$3c^2$	$\frac{3}{4}c^4$	(0,0) $(\cos\frac{2\pi a}{6}, \sin\frac{2\pi a}{6})$
D_2Q_9 Fig.1a	4^{th}	3	$w_0 = var = \{\frac{4}{9}\}$ $w_a^{orth} = 4w_a^{diag}$ $w_a^{diag} = \frac{1-w_0}{20}$	$\frac{3(1-w_0)}{5}c^2$	$\frac{1-w_0}{5}c^4$	(0,0) cyc.$(\pm 1, 0)$ $(\pm 1, \pm 1)$
D_3Q_{15} Fig.1b	4^{th}	3	$w_0 = var = \{\frac{1}{8}\}$ $w_a^{orth} = 8w_a^{diag}$ $w_a^{diag} = \frac{1-w_0}{56}$	$\frac{3(1-w_0)}{7}c^2$	$\frac{1-w_0}{7}c^4$	(0,0,0) cyc.$(\pm 1, 0, 0)$ $(\pm 1, \pm 1, \pm 1)$

[a] $D_{\mathcal{D}}Q_{b+1}$, where $\mathcal{D}$ is a dimension and b is the total number of moving directions.

[b] The most commonly used values are given in brackets.

[c] Note: $\sum_a w_a = 1$.

[d] $c = \frac{\delta_x}{\delta_t}$, where δ_x and δ_t are length and time scales, correspondingly.

[e] Note that the pressure constitutes the diagonal part of the fluid's stress tensor. Thus, the coefficient before the second-order Kroenecker symbol $\delta_{i,j}$ is the lattice sound speed, $\Upsilon^{(2)} \equiv c_s^2$.

The equilibrium distribution function may be approximated by series of Chapman-Enskog expansions in macroscopic variables, to the second order, in the low-Mach-number limit:

$$f_{a\neq 0}^{\mathrm{eq}} = \rho w_a \left[A + Be_{a_i}u_i + Cu^2 + De_{a_i}e_{a_j}u_iu_j + ...\right] \qquad \text{(B.2)}$$
$$f_0^{\mathrm{eq}} = \rho w_0 \left[A_0 + C_0u^2 + ...\right]$$

Using the symmetry properties of the lattice given in appendix A, one can show that the constraints eq.(B.1) are satisfied with the following parameters of the expansion:

$$A + Cu^2 = \frac{2c_s^2 - u^2}{2\Upsilon^{(2)}} + \beta \qquad \text{(B.3)}$$

$$B = \frac{1}{\Upsilon^{(2)}} \qquad \text{(B.4)}$$

$$Du_iu_j = \frac{u_iu_j}{2\Upsilon^{(4)}} + \frac{1}{2\rho\Upsilon^{(4)}}\left[P_{ij}^{\star} - \frac{Tr(P^{\star})}{2+\mathcal{D}}\delta_{ij} - \rho\beta\Upsilon^{(2)}\frac{2}{2+\mathcal{D}}\delta_{ij}\right] \qquad \text{(B.5)}$$

$$A_0 + C_0u^2 = \frac{1}{w_0}\left[1 - (1-w_0)\frac{2c_s^2 - u^2}{2\Upsilon^{(2)}} - \frac{u^2\Upsilon^{(2)}}{2\Upsilon^{(4)}} - \right. \qquad \text{(B.6)}$$

$$-\frac{\frac{\Upsilon^{(2)}}{\Upsilon^{(4)}(2+\mathcal{D})}\left[Tr(P^\star)-\rho\beta\mathcal{D}\Upsilon^{(2)}\right]-\rho\beta(1-w_0)}{\rho}\Bigg] \tag{B.7}$$

where β is a free parameter left, $\mathcal{D}$ is a space dimension, and $Tr(P^\star)$ is a trace of the nonideal part of the pressure tensor, $P^\star_{i,j}=P_{i,j}-\rho c_s^2\delta_{i,j}$.

Coefficient $\mathcal{M}$ is given by:

$$\mathcal{M}=\rho\frac{\Upsilon^{(4)}}{\Upsilon^{(2)}} \tag{B.8}$$

Setting $\beta=0$ and $P^\star_{i,j}=0$ ('ideal fluid'), we can write $f_a^{\rm eq}$ in the following compact form:

$$\begin{aligned} f_0^{\rm eq}&=\rho\left[1-\frac{1-w_0}{\Upsilon^{(2)}}c_s^2-\frac{u^2}{2}\left(\frac{\Upsilon^{(2)}}{\Upsilon^{(4)}}-\frac{1-w_0}{\Upsilon^{(2)}}\right)\right]\\ f_{a\neq0}^{eq,0}&=\rho w_a\left[\frac{c_s^2}{\Upsilon^{(2)}}-\frac{u^2}{2\Upsilon^{(2)}}+\frac{e_{a_i}u_i}{\Upsilon^{(2)}}+\frac{e_{a_i}e_{a_j}u_iu_j}{2\Upsilon^{(4)}}\right] \end{aligned} \tag{B.9}$$

which are exactly the same equations as given in the LBE literature, [12] and [63].

Using the pressure tensor given by eq.(75) and the following equation for β:

$$\beta=\frac{P_0^\star-\kappa\rho\partial_{kk}\rho+\left(\frac{1}{\mathcal{D}}-\frac{1}{2}\right)\kappa\left(\partial_k\rho\right)^2}{\Upsilon^{(2)}\rho} \tag{B.10}$$

where $P_0^\star=P_0-\rho c_s^2$ is a 'nonideal part' of the equation of state, we arrive to the 'free-energy-based' lattice Boltzmann model for 'non-ideal fluid' by Swift et al. [78].

Notably, that for 'ideal fluid' model the speed of sound is a function of the lattice space and time scales, δ_x and δ_t, and the weight of the non-moving populations w_0, see Table 1. Setting $w_0=\frac{4}{9}$ for the D_2Q_9, one can get the non-dimensionalized sound speed of the lattice, $\left(\frac{c_s}{c}\right)^2=\frac{1}{3}$, the value which is widely used in the literature of the LBE theory [63].

APPENDIX C

Derivation of the viscous stress tensor for the LBGK models

Isothermal ideal gas.

$$\begin{aligned} \partial_j\mathcal{T}^{\rm LBGK}_{i,j}&=-\partial_j\varepsilon\mathcal{P}^{(1)}_{i,j}=-\partial_j\varepsilon\underbrace{\sum_a(e_{a_i}-u_i)(e_{a_j}-u_j)f_a^{(1)}}_{\mathcal{P}^{(1)}_{i,j}=\sum_a e_{a_i}e_{a_j}f_a^{(1)}}=\\ &=\left[...f_a^{(1)}=\ \text{eq.(54)}\ =-\tau\left(\partial_{t_0}f_a^{(0)}+e_{a_k}\partial_k f_a^{(0)}-\tfrac{a_k}{c_s^2}(e_{a_k}-u_k)f_a^{(0)}\right)...\right]=\\ &=\tau\varepsilon\partial_j\left(\underbrace{\partial_k\mathcal{D}^{(0)}_{i,j,k}}_{\rm (A)}+\underbrace{\partial_{t_0}\Pi^{(0)}_{i,j}}_{\rm (B)}-\underbrace{\frac{a_k}{c_s^2}\left(\mathcal{D}^{(0)}_{i,j,k}-u_k\Pi^{(0)}_{i,j}\right)}_{\rm (C)\to A_{i,j}=Artifact}\right) \end{aligned} \tag{C.1}$$

The $\mathcal{D}^{(0)}_{i,j,k}$ and $\Pi^{(0)}_{i,j}$ are given by eq.(B.1).

$$\begin{aligned}(\mathrm{A}): \quad \partial_j\partial_k\left[\underbrace{\tau\varepsilon\rho\frac{\Upsilon^{(4)}}{\Upsilon^{(2)}}}_{=\hat{\mathcal{M}},\ \text{eq.(B.8)}}\left(u_i\delta_{j,k}+u_j\delta_{i,k}+u_k\delta_{i,j}\right)\right] = \\ = \underbrace{\partial_j\left[\hat{\mathcal{M}}\left(\partial_j u_i+\partial_i u_j\right)+\hat{\mathcal{M}}\cdot\partial_k u_k\cdot\delta_{i,j}\right]}_{\to\mathcal{T}_{i,j}=\text{N.S. viscous stress tensor}}+\underbrace{\partial_j\left[u_i\partial_j\hat{\mathcal{M}}+u_j\partial_i\hat{\mathcal{M}}+u_k\cdot\partial_k\hat{\mathcal{M}}\cdot\delta_{i,j}\right]}_{\to\mathsf{A}_{i,j}=\text{Artifact}}\end{aligned} \tag{C.2}$$

At this stage, we can identify shear viscosity as

$$\eta=\hat{\mathcal{M}}=\tau\varepsilon\rho\tfrac{\Upsilon^{(4)}}{\Upsilon^{(2)}} \tag{C.3}$$

and

$$\tau\varepsilon=\nu\tfrac{\Upsilon^{(2)}}{\Upsilon^{(4)}},\quad \nu=\tfrac{\eta}{\rho}=\text{const} \tag{C.4}$$

$$\begin{aligned}(\mathrm{B}): \quad \nu\tfrac{\Upsilon^{(2)}}{\Upsilon^{(4)}}\partial_j\left[\underbrace{c_s^2\partial_{t_0}\rho\delta_{i,j}}_{-c_s^2\partial_k\rho u_k\delta_{i,j},\ \text{eq.(48)}}+\ \partial_{t_0}\rho u_i u_j\right] = \\ = \nu\tfrac{\Upsilon^{(2)}}{\Upsilon^{(4)}}\partial_j\left[\underbrace{-\rho c_s^2\partial_k u_k\delta_{i,j}}_{\to\mathcal{T}_{i,j}}\underbrace{-c_s^2u_k\partial_k\rho\delta_{i,j}}_{\to\mathsf{A}_{i,j}}+\underbrace{u_i\underbrace{\partial_{t_0}\rho u_j}_{\text{eq.(49)}}+u_j\underbrace{\partial_{t_0}\rho u_i}_{\text{eq.(49)}}}_{\to\mathsf{A}_{i,j}}\right]\end{aligned} \tag{C.5}$$

Combining all terms, the viscous stress tensor is given by

$$\partial_j\mathcal{T}^{\mathrm{LBGK}}_{i,j}=\partial_j\left[\eta\left(\partial_j u_i+\partial_i u_j\right)+\left(\eta-\eta c_s^2\tfrac{\Upsilon^{(2)}}{\Upsilon^{(4)}}\right)\partial_k u_k\cdot\delta_{i,j}\right] \tag{C.6}$$

yielding the second viscosity given by eq.(64). The rest terms are agglomerated into the 'artifact' tensor:

$$\begin{aligned}\mathsf{A}_{i,j}=\nu\partial_j\left[u_i\partial_j\rho+u_j\partial_i\rho+u_k\partial_k\rho\delta_{i,j}\right]+ \\ +\nu\tfrac{\Upsilon^{(2)}}{\Upsilon^{(4)}}\partial_j\left[-c_s^2u_k\partial_k\rho\delta_{i,j}+u_i\left(-\partial_k\rho u_k u_j-c_s^2\partial_j\rho+\rho a_j\right)+\right. \\ \left.+u_j\left(-\partial_k\rho u_k u_i-c_s^2\partial_i\rho+\rho a_i\right)\right. \\ \left.-\tfrac{a_k}{c_s^2}\left(\rho\tfrac{\Upsilon^{(4)}}{\Upsilon^{(2)}}\left(u_i\delta_{j,k}+u_j\delta_{i,k}+u_k\delta_{i,j}\right)-u_k\left(\rho c_s^2\delta_{i,j}+\rho u_i u_j\right)\right)\right]\end{aligned} \tag{C.7}$$

which, setting $\frac{\Upsilon^{(4)}}{\Upsilon^{(2)}}=c_s^2$, can be further re-arranged to produce the non-linear deviation term given by eq.(61).

Free-energy-based model for non-ideal fluid. Repeating the calculations presented above[43], the following viscosities and "artifact" terms are obtained:

$$\eta = \tau\varepsilon\rho\frac{\Upsilon^{(4)}}{\Upsilon^{(2)}};\ \xi = \eta\left(\frac{5}{3} + \frac{\Upsilon^{(2)}}{\Upsilon^{(4)}}\left(2\mathsf{a}\rho - \frac{c_s^2}{1-\mathsf{b}\rho} - \frac{\rho c_s^2\mathsf{b}}{(1-\mathsf{b}\rho)^2} + \kappa\partial_l^2\rho\right)\right) \quad \text{(C.8)}$$

$$\begin{aligned}\mathsf{A}_{i,j} = \nu\tfrac{\Upsilon^{(2)}}{\Upsilon^{(4)}}\Big\{\partial_j\Big[\Big(\Big(2\mathsf{a}\rho - \tfrac{c_s^2}{1-\mathsf{b}\rho} - \tfrac{\rho c_s^2\mathsf{b}}{(1-\mathsf{b}\rho)^2}\Big)u_k + \kappa\left(u_k\partial_l^2\rho + \partial_{kl}\rho u_l\right)\Big)\partial_k\rho\delta_{i,j}\\ -\partial_i\rho\left[\kappa\partial_{jk}\rho u_k + u_j\left(\tfrac{c_s^2}{1-\mathsf{b}\rho} + \tfrac{\rho c_s^2\mathsf{b}}{(1-\mathsf{b}\rho)^2}\right) - 2\mathsf{a}\rho u_j\right] -\\ -\partial_j\rho\left[\kappa\partial_{ik}\rho u_k + u_i\left(\tfrac{c_s^2}{1-\mathsf{b}\rho} + \tfrac{\rho c_s^2\mathsf{b}}{(1-\mathsf{b}\rho)^2}\right) - 2\mathsf{a}\rho u_i\right] - \partial_k\rho\cdot 2u_iu_ju_k\Big] -\\ -\left[u_i\partial_k u_k u_j + u_j\partial_k u_k u_i\right]\cdot\partial_j\rho\Big\} - \eta\tfrac{\Upsilon^{(2)}}{\Upsilon^{(4)}}\partial_j\left[u_i\partial_k u_k u_j + u_j\partial_k u_k u_i\right]\end{aligned} \quad \text{(C.9)}$$

"HSD" model for non-ideal fluid. The following "artifact" term is obtained for the "HSD" model:

$$\begin{aligned}\mathsf{A}_{i,j} = -\nu\tfrac{\Upsilon^{(2)}}{\Upsilon^{(4)}}\Big\{\partial_j\Big[\Big(c_s^2 - \tfrac{\Upsilon^{(4)}}{\Upsilon^{(2)}}\Big)\left(u_k\partial_k\rho\delta_{i,j} + u_i\partial_j\rho + u_j\partial_i\rho\right) -\\ -\Big(2\mathsf{a}\rho + c_s^2 - \tfrac{c_s^2}{1-\mathsf{b}\rho} - \tfrac{\rho c_s^2\mathsf{b}}{(1-\mathsf{b}\rho)^2}\Big)\Big(\tfrac{u_iu_ju_k}{c_s^2}\partial_k\rho + \Big(1 - \tfrac{\Upsilon^{(4)}}{\Upsilon^{(2)}c_s^2}\Big)\cdot\\ \cdot\left(u_i\partial_j\rho + u_j\partial_i\rho + u_k\partial_k\rho\delta_{i,j}\right)\Big) - \rho\kappa\left[u_i\partial_j^3\rho + u_j\partial_i^3\rho + \partial_k\partial_l^2\rho\cdot\right.\\ \left.\cdot\Big(u_k\Big(1 - \tfrac{\Upsilon^{(4)}}{\Upsilon^{(2)}c_s^2}\Big)\delta_{i,j} + \tfrac{u_iu_ju_k}{c_s^2}\Big) - \tfrac{\Upsilon^{(4)}}{\Upsilon^{(2)}c_s^2}\left(u_i\partial_j\partial_k^2\rho + u_j\partial_i\partial_k^2\rho\right)\right] +\\ +2u_iu_ju_k\partial_k\rho] -\\ -\partial_j\rho\left[\Big(1 - \tfrac{\Upsilon^{(4)}}{\Upsilon^{(2)}c_s^2}\Big)\left(u_ig_j + u_jg_i + u_kg_k\delta_{i,j}\right) + \tfrac{u_iu_ju_k}{c_s^2}g_k - u_i\partial_k u_ju_k - u_j\partial_k u_iu_k\right]\Big\} +\\ +\eta\partial_j\left[\Big(\tfrac{\Upsilon^{(2)}}{\Upsilon^{(4)}} - \tfrac{1}{c_s^2}\Big)\left(u_ig_j + u_jg_i + u_kg_k\delta_{i,j}\right)\right.\\ \left.+\tfrac{\Upsilon^{(2)}}{\Upsilon^{(4)}}\Big(\tfrac{u_iu_ju_kg_k}{c_s^2} - u_i\partial_k u_ju_k - u_j\partial_k u_iu_k\Big)\right]\end{aligned} \quad \text{(C.10)}$$

[43] In this derivation though, for simplicity, we neglected the derivatives of the third and higher order. Strictly speaking, this is not well grounded, because the momentum conservation equation (77) contains terms of the third-order derivative of density.